Journal of Hydrology: Regional Studies 59 (2025) 102347

Contents lists available at ScienceDirect

Journal of Hydrology: Regional Studies

journal homepage: www.elsevier.com/locate/ejrh

Long-term hydroclimate trends in the Great Lakes basin: Are there hotspots of regional change?

Satbyeol Shin [a,d,*], Andrew D. Gronewold [a], Lauren M. Fry [b], Yi Hong [c], David Cannon [c], Ayumi Fujisaki-Manome [c,e]

[a] *School for Environment and Sustainability, University of Michigan, Ann Arbor, MI, USA*
[b] *NOAA Great Lakes Environmental Research Laboratory, Ann Arbor, MI, USA*
[c] *Cooperative Institute for Great Lakes Research, University of Michigan, Ann Arbor, MI, USA*
[d] *Department of Civil and Environmental Engineering, Yonsei University, Seoul, South Korea*
[e] *Climate & Space Sciences and Engineering, University of Michigan, Ann Arbor, MI, USA*

ARTICLE INFO

Keywords:
Historical changes
Seasonal shifts
Hydrological modeling
Apportionment entropy

ABSTRACT

Study Region: The Laurentian Great Lakes basin
Study focus: This study analyzed key hydroclimate components across the entire Laurentian Great Lakes basin, one of the largest freshwater basins on Earth and home to roughly 20% of all fresh, unfrozen surface water. The hydroclimate components analyzed included surface air temperature, precipitation, evapotranspiration (ET), snow water equivalent (SWE), runoff, and surface soil moisture from 1951 to 2020. Hydrological variables were simulated using regional customization of the Weather Research and Forecasting hydrological model (WRF-Hydro), and changes in the annual magnitude and seasonal variability (i.e. seasonality) of all variables were assessed.
New hydrological insights for the region: Our findings reveal significant spatial and temporal variations in hydroclimate variables across the basin. The Great Lakes basin is experiencing noteworthy changes in hydroclimate variables, including pronounced rises in surface air temperature, ET, and runoff (low flow), as well as declines in SWE. The distinct spatial patterns of changes in magnitude and seasonality are identified throughout the region. For instance, the Superior basin exhibits unique hydrological patterns, including an earlier peak in SWE and decreased high flow, both of which are influenced by its unique climatic and geographical conditions. This long-term analysis of hydroclimate trends provides valuable insights into historical hydrological changes and their implications for future conditions in the Great Lakes basin, emphasizing the need for localized studies and targeted management strategies.

1. Introduction

Understanding long-term historical hydroclimate changes in a region is crucial, particularly in the context of a changing climate (Stevenson et al., 2022). A comprehensive, long-term retrospective analysis of hydrological simulations provides a vital reference point for studying future hydroclimatic conditions. In order to effectively anticipate future scenarios, it is imperative to establish a baseline that accurately reflects historical hydroclimate conditions. For example, thorough assessments of historical hydroclimate conditions

* Corresponding author at: School for Environment and Sustainability, University of Michigan, Ann Arbor, MI, USA.
E-mail address: satshin@umich.edu (S. Shin).

https://doi.org/10.1016/j.ejrh.2025.102347
Received 15 January 2025; Received in revised form 23 March 2025; Accepted 25 March 2025
Available online 9 April 2025
2214-5818/

are essential prior to integrating them into hydrological models for future scenarios (Johnson and Sharma, 2009; Woldemeskel et al., 2016; Song et al., 2020; Shin et al., 2023a). This research aims to enhance our comprehension of historical regional trends within the unique and complex transboundary region of the North American Laurentian Great Lakes basin. By focusing on a baseline that most accurately captures real historical changes, we can better interpret baseline simulations and, as a result, have greater confidence in future climate projections.

Hydrological changes across the Great Lakes and their drainage basins are particularly important given concerns about the potential impacts of future climate (Byun et al., 2019; Mailhot et al., 2019; Soonthornrangsan and Lowry, 2021; Kayastha et al., 2022; Myers et al., 2023; Pal et al., 2023). The Great Lakes basin holds approximately 20% of the world's surface freshwater (Gronewold et al., 2013; 2019). Due to the region's importance as a highly populated transboundary river basin, numerous studies have investigated hydrological responses to climate change in the Great Lakes. These studies have explored topics such as lake warming (Mason et al., 2016; Cannon et al., 2024), water balance (Gronewold et al., 2013), hydrologic extremes (Byun et al., 2019), compound floods in coastal regions (Hong et al., 2024), vulnerability of water resources (Soonthornrangsan and Lowry, 2021), the impacts of land-use changes on hydrologic responses (Kult et al., 2014; Mao and Cherkauer, 2009), and projected rain-on-snow melt events (Myers et al., 2023). While each study provides unique insights into hydrological processes in the Great Lakes region, none have examined long-term historical hydroclimate trends for the entire Great Lakes drainage basin. Only a select few (Mailhot et al., 2019; Kayastha et al., 2022; Shrestha et al., 2022; Myers et al., 2023) have considered the entire Great Lakes basin; however, these studies have not covered a sufficiently long historical period to provide insights into long-term hydroclimate trends. What's more the spatial resolution of hydrological models used in these studies is too coarse (e.g., lumped or semi-distributed unit at the subbasin scale) to consider interactions between the land surface and hydrological processes.

Hydrological models are essential tools for water resources management and planning, and the increasing spatial and temporal resolution of these models is resulting in a more comprehensive understanding of diverse hydrological processes, including the identification of potential environmental and climate hot spots (Bierkens et al., 2015; Clark et al., 2015; Fatichi et al., 2016). Though historical hydrological conditions can be assessed using ground-based or remotely sensed data, each method has limitations. In-situ measurements are often limited by ungauged areas and sparse spatial and temporal resolution (Balsamo et al., 2018; Shin et al., 2023b), and remotely sensed products, being relatively new, generally do not cover multi-decadal historical time scales and require robust validation against in-situ measurements (Moradkhani, 2008; Dong, 2018). Moreover, individual data sources cannot fully capture interactions between atmospheric, land surface, and hydrological processes, though they serve as valuable supplementary datasets to assess hydrologic model skill (Ragettli et al., 2015; Rajib et al., 2016; Balsamo et al., 2018). Hydrological models, especially high-resolution modeling at large scales, therefore serve as a well-established tool for bridging gaps in historical data while also offering potential additional insights into the complexities of hydrological processes (Fatichi et al., 2016; Shin et al., 2023b). As fundamental tools for water management, they also enable decision-makers to develop effective strategies for sustainable and responsible water resource management, providing a holistic understanding of hydrological dynamics.

Numerous studies have analyzed long-term hydrological trends using various modeling approaches, including data-driven methods (Kult et al., 2014; Ljungqvist et al., 2016; Adnan et al., 2024), lumped models (Chen et al., 2007; Wu et al., 2014), semi-distributed models (Nijssen et al., 2001; Wu and Johnston, 2007), and fully-distributed models (Pal et al., 2023), but are not limited to these approaches. Many of these studies employ computationally efficient models, which are well-suited for analyzing hydrological processes over multi-decadal periods. However, these models often simplify hydrological processes and operate at relatively coarse spatial resolution, which can potentially miss important localized hydrological dynamics. The application of complex, hyper-resolution hydrological models for long-term trend analysis remains limited. The advanced models offer high-resolution capabilities and a more detailed representation of hydrological processes. However, they come with challenges, including high computational demands and significant storage requirements for inputs and outputs, which have limited their use in long-term studies.

This study tests the two hypotheses: first, there are distinct environmental hotspots where hydroclimate processes are significantly changing across the Great Lakes basin, and second, the magnitude and direction of long-term changing trends in various hydroclimate variables differ. In order to test these assumptions, this study investigated comprehensive long-term hydroclimate changes across the entire Great Lakes basin from 1951 to 2020, to identify environmental hot spots, annual and seasonal trends, and interrelationships between hydroclimate components – such as surface air temperature, precipitation, evapotranspiration (ET), snow water equivalent (SWE), runoff (considered as routed runoff or streamflow), and surface soil moisture. Previous studies have been limited either by their focus on short-term periods for the whole region or by long-term analyses for only portions of the basin, and they have not employed fine-resolution hydrological models. Our work fills these gaps by utilizing a fully-distributed hyper-resolution land surface hydrological model, the Weather Research and Forecasting Hydrological model (WRF-Hydro; Gochis et al., 2020), to conduct 70 years of retrospective simulations in the Great Lakes basin with recent 20-year outputs compared against various in-situ measurements and remote sensing products. This approach allows us to examine environmental hot spots at different spatial scales (e.g., lake basins and subbasins) and temporal scales (e.g., annual and seasonal) and analyze trends in extreme conditions. The novelty of this study lies in its extensive spatial and temporal scope, offering valuable insights into historical hydroclimate changes across the entire Great Lakes region. The findings of this study provide implications for the development of effective water resource management strategies in the Great Lakes region and other areas with similar hydroclimate dynamics.

2. Methods

2.1. Great Lakes Basin

The North American Laurentian Great Lakes basin includes the largest system of lakes on Earth and is one of the largest transboundary watersheds, encompassing parts of both the United States and Canada and multiple other sovereign tribal nations. Over 30 million people live in the Great Lakes basin, relying on the lakes for drinking water, transportation, recreation, and industry (Gronewold et al., 2013; Méthot et al., 2015; Sterner et al., 2020). It is common for the Great Lakes to be analyzed at lake basin scales (i.e. for the basins of Lake Superior, Michigan-Huron, Erie, and Ontario), as shown in Fig. 1 (Hong et al., 2022). It is less common for spatial variability to be assessed across the region's subbasins (Fig. 1), which are often utilized for regional hydrological modeling and water supply forecasting (Croley, 2002; Gronewold et al., 2011; Gronewold and Fortin, 2012; Fry et al., 2014; Gaborit et al., 2017).

The Great Lakes basin covers a total surface area of 717,797 km^2, of which about 35% is the surface area of the lakes themselves (see Figure S1 in the Supplementary Materials). The land elevation across the basin ranges from 75 to 800 m above mean sea level (m a.s.l.), with an average elevation of 260 m a.s.l. The dominant land uses are forest (27%) and cropland (18%), with most forests located in the northern parts of the region and most cropland in the southern parts (Figure S1). Soil texture varies throughout the basin; sandy loam is dominant in the northern parts, including the Superior, Michigan-Huron, and northern Ontario basins, while silt loam is dominant in the southern parts, where the Erie and southern Ontario basins are located (Figure S1; see Data Availability for detailed information of the land surface datasets).

2.2. Land surface and hydrological modeling

WRF-Hydro was used to analyze long-term hydroclimate trends in the Great Lakes basin. Originally developed by the National Center for Atmospheric Research (NCAR). This model simulates land surface energy and hydrological fluxes, with options to either couple with regional atmospheric models (e.g. WRF) or use external meteorological forcing datasets (i.e., in uncoupled or standalone mode) with land surface modeling (Gochis et al., 2020). WRF-Hydro allows users to choose between two 1-dimensional column land surface models: Noah (Ek et al., 2003) and Noah Multiparameterization (Noah-MP; Niu et al., 2011), which both simulate vertical fluxes of energy and moisture in the land surface. Each column of the model has a fixed 2-meter soil depth, divided into four layers with thicknesses of 0.1, 0.3, 0.6, and 1.0 m from the surface to the bottom, respectively. The model uses the Penman-Monteith equation (Monteith, 1965) to calculate ET, connecting the water and energy balance equations (Cai et al., 2014; Duan and Kumar, 2020), and employs the 1-dimensional diffusive form of Richard's equation for vertical water movement within the soil layers (He et al., 2023). These land surface processes are dynamically coupled with terrestrial hydrological processes, representing surface, subsurface,

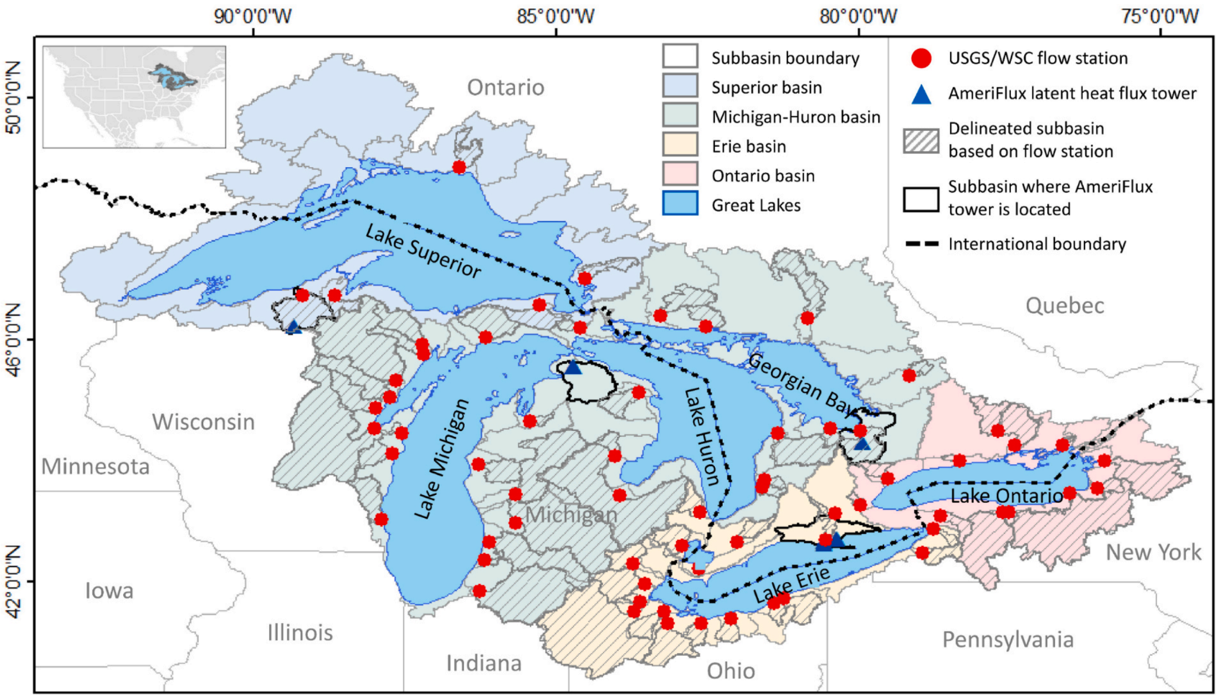

Fig. 1. Map of the Great Lakes basin with locations of the in-situ measurements for streamflow (the United States Geological Survey (USGS) and Water Survey of Canada (WSC) gages) and latent heat flux (AmeriFlux tower). Colors differentiate individual lake basins, and subbasins are delineated within each lake basin.

channel routing, and groundwater systems.

In this study, we employed WRF-Hydro in standalone mode with the Noah-MP land surface model. The hydrological routing options of the steepest descent method and the Muskingum-Cunge method were selected to represent surface overland flow routing and reach-based channel routing, respectively. We used the configuration and calibrated parameter sets of the National Water Model version 2.1 (NWMv2.1) for the WRF-Hydro simulation. The NWM was originally calibrated by NCAR and further refined by the NOAA Great Lakes Environmental Research Laboratory using an updated spatially consistent hydrofabric dataset for the Canadian portion of the Great Lakes (Mason et al., 2019). NWMv2.1 was calibrated and validated for the period from 2008 to 2016, focusing on streamflow with the meteorological forcing of the Analysis of Record for Calibration (AORC; Fall et al., 2023) dataset (Cosgrove et al., 2024).

We used the fifth-generation European Centre for Medium-Range Weather Forecasts atmospheric reanalysis data (ERA5; Hersbach et al., 2018) as an external forcing of WRF-Hydro in standalone mode instead of the original AORC forcing. This choice was due to ERA5's longer data record (ERA5 is available from 1940 onwards, whereas AORC is available from 1979) and its well-documented and more widely used presence in the peer-reviewed literature (Shin et al., 2024). ERA5 provides data on precipitation, surface air temperature, surface pressure, specific humidity, short and long wave radiation, and wind speed (zonal and meridional directions) with a spatial resolution of 0.25° and a temporal resolution of hourly. This study employed spatial datasets including digital elevation maps, soil maps, land use, and river networks for model setup (see Data Availability). The hydrofabric dataset for the entire Great Lakes basin, customized by Mason et al. (2019), seamlessly combines hydrographic data from the United States and Canada and is incorporated into NWMv2.1. The meteorological forcing dataset and spatial inputs were regridded to a 1 km resolution. The modeling outputs are provided at a 1 km/daily resolution (Shin and Gronewold, 2024).

We evaluated the model accuracy for streamflow as well as auxiliary hydrological variables such as ET, SWE, and surface soil moisture. The model evaluation was conducted for the period from 2001 to 2020 using Kling-Gupta Efficiency (KGE; Gupta et al., 2009) and Percentage Bias (PBIAS) comparing the simulations against various reference datasets including in-situ measurements and remote sensing products (Table 1 and Fig. 1). KGE and PBIAS are widely used error metrics that evaluate hydrological model performance (Huang et al., 2017; Althoff and Rodrigues, 2021; Mai et al., 2022). KGE integrates different error components such as correlation, bias, and variability (Eq. 1), and ranges from -∞ to 1, where negative values indicate an unreliable model, while values closer to 1 represent reliable. On the other hand, PBIAS measures the systematic overestimation and underestimation of a model by calculating the difference between observed and simulated values (Eq. 2). PBIAS values closer to zero indicate better model accuracy, while higher absolute values suggest greater bias in model predictions.

$$KGE = 1 - \sqrt{(r-1)^2 + (\beta-1)^2 + (\gamma-1)^2} \tag{1}$$

Table 1
Summary of model inputs and references for output evaluation.

Type	Item			Data period	Number of subbasins covered	Spatial/temporal resolution
Model inputs	Spatial data	Topography	NED[a]	–	All	1 arc-second/–
		Reach	NHD Plus V2[b]	–	All	1 arc-second/–
		Land use	NLCD[c]	–	All	30 m/–
		Soil	STATSGO[d]	–	All	1 km/–
	Climate data		ERA5[e]	1940 – 2020	All	0.25°/hour
Reference for output evaluation	ET		GLEAM[f]	1980 – 2020	All	0.25°/day
			MODIS[g]	2002 – 2020	All	500 m/8-day
			AmeriFlux[h]	Vary	4 (8 stations), Fig. 1	Point/30-min
	SWE		CMC[i]	1998 – 2020	All	0.33°/month
	Runoff		USGS and WSC[j]	2000 – 2020	65, Fig. 1	Point/day
	Soil moisture		GLEAM	1980 – 2020	All	0.25°/day

[a] NED: National Elevation Dataset (NED; Gesch et al., 2002).
[b] NHD Plus V2: National Hydrography Dataset Plus V2 (NHD Plus V2; McKay et al., 2012).
[c] NLCD: National Land Cover Database (NLCD; Homer et al., 2015).
[d] STATSGO: State Soil Geographic (STATSGO; Miller and White, 1998).
[e] ERA5: The fifth-generation European Centre for Medium-Range Weather Forecasts atmospheric reanalysis data (ERA5; Hersbach et al., 2018).
[f] GLEAM: Global Land Evaporation Amsterdam Model (GLEAM; Martens et al., 2017), a Satellite-based modeling product.
[g] MODIS: Moderate Resolution Imaging Spectroradiometer (MODIS; Running et al., 2017), a Satellite-based modeling product.
[h] AmeriFlux: In-situ measurements collected from the AmeriFlux towers. The AmeriFlux towers employed in this study are CA-Cbo (Staebler, 2022) for the subbasin GEO03, CA-TP1 (Arain, 2018a), CA-TP3 (Arain, 2018b), CA-TP4 (Arain, 2018c), and CA-TPD (Arain, 2018d) for the subbasin ERI20, US-Syv (Desai, 2023) for the subbasin SUP05, US-UMB (Gough et al., 2023a), and US-UMd (Gough et al., 2023b) for the subbasin HUR03. The available data period for each station varied from 1995 to 2020.
[i] CMS: Canadian Meteorological Centre (CMC; Brown and Brasnett, 2010), in-situ snow depths measurements and optimal interpolation using a simple snow accumulation and melt model.
[j] USGS and WSC: In-situ measurements collected from the United States Geological Survey (USGS; (https://waterdata.usgs.gov/nwis/rt) and Water Survey of Canada (WSC; https://wateroffice.ec.gc.ca/search/historical_e.html) stations.

$$PBIAS = \left[\sum_{i=1}^{n} (O_i - m_i)^2 \Big/ \sum_{i=1}^{n} {O_i}^2 \right] \times 100\% \tag{2}$$

where, r is correlation coefficient between observed and simulated values (measuring linear association), β is bias ratio, defined as $\frac{\mu_m}{\mu_o}$ where, μ_m and μ_o are the means of modeled and observed values, respectively (measuring systematic bias), γ is variability ratio, defined as $\frac{\sigma_m/\mu_m}{\sigma_o/\mu_o}$ where, σ_m and σ_o are the standard deviations of modeled and observed values, respectively (measuring relative variability). n is the total number of observations, and O_i and m_i is the i^{th} observed and modeled data, respectively.

We collected three kinds of ET reference datasets, two of them are remote sensing products from the Global Land Evaporation Amsterdam Model (GLEAM; Martens et al., 2017) and the Moderate-Resolution Imaging Spectroradiometer (MODIS; Running et al., 2017) and one is in-situ dataset collected from 8 AmeriFlux sites (see Table 1). Remote sensing data can cover all of the Great Lakes region, but the in-situ dataset for ET can cover only 4 subbasins (Fig. 1). For the SWE reference data, we collected a remote-sensing product provided by the Canadian Meteorological Centre (CMC; Brown and Brasnett, 2010). For the runoff reference data, we obtained in-situ streamflow measurements from the United States Geological Survey (USGS) and Water Survey of Canada (WSC) stations, which can cover 65 subbasins over the Great Lakes basins. Most reference datasets can cover the recent 20 years.

As the reference data and model outputs have different spatiotemporal resolutions (Table 1), first spatial aggregation of the model outputs (e.g., 1 km) and reference datasets into subbasin averages was conducted to reduce errors induced by spatial interpolation of the reference data (Ma et al., 2017). Satellite-based products were aggregated into subbasin-wide averages directly, whereas in-situ measurements—such as ET from AmeriFlux and streamflow from USGS/WSC—required tailored approaches. For ET, only four subbasins were covered by AmeriFlux towers (Fig. 1), so average values were computed for the available datasets under the assumption that each represents its corresponding subbasin. For runoff, a watershed boundary was delineated based on each streamflow gauge (Fig. 1), with the gauged flow assumed to represent the delineated area, and the average of the model outputs for these areas was compared accordingly. Then, temporal upscaling–from half-hourly (AmeriFlux), daily (WRF-Hydro, GLEAM, USGS/WSC), and 8-day (MODIS) intervals–to monthly scale was conducted, enabling a direct comparison between the model outputs and reference data for the period from 2001 to 2020.

2.3. Long-term trend analysis

The hydroclimate change analysis utilized climate variables including surface air temperature and precipitation directly from the ERA5 dataset, while hydrological variables include ET, SWE, runoff, and surface soil moisture from the WRF-Hydro simulation. For the WRF-Hydro simulation, the initial 11 years from 1940 to 1950 were used as a spin-up to stabilize initial conditions, and the subsequent 70 years of simulations were used to analyze long-term hydroclimate trends in the Great Lakes basin (more details on the model structure, parameters, and input data are available in Section 2.2). The modeling outputs (1 km/daily) were aggregated to subbasin-wide or lake-basin-wide averages (Fig. 1) with monthly or annual scales. Based on hydroclimate components from ERA5 dataset and WRF-Hydro simulation, the annual and seasonal trends, multidecadal changes, and interrelationships between hydroclimate components were analyzed (Fig. 2).

We applied the Mann-Kendall trend test to annual time series to identify significant monotonic trends (p-value less than 0.05) and calculated Sen's slope estimator (Sen, 1968) to estimate the changing magnitudes. Additionally, we investigated lake-basin-wide monthly climatology to examine the seasonality of each hydroclimate component. In this study, seasonality refers to recurring temporal patterns observed in monthly time-series data. Then, subbasin-wide changing trends for annual magnitudes and seasonalities were assessed to identify hotspots for each hydroclimate variable. For trends in annual magnitude, Sen's slope estimator of the annual time series for each hydroclimate component was calculated at each subbasin. For changes in annual seasonality, we employed a non-parametric estimator, the apportionment entropy (AE; Mishra et al., 2009; Konapala et al., 2020), and its change ratio represented in units of percentage change per decade (Stahl et al., 2012).

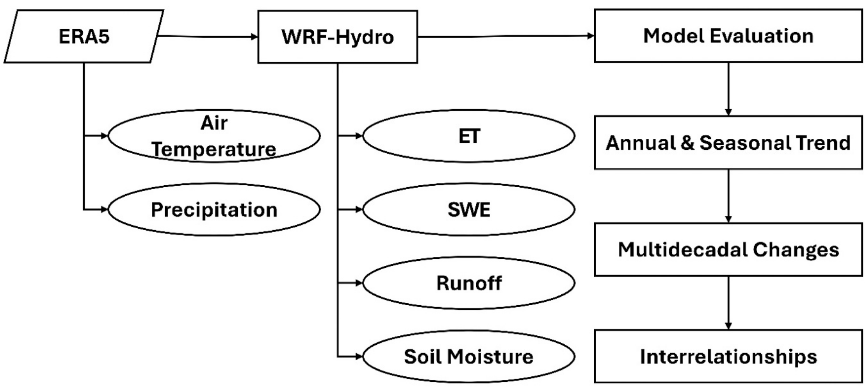

Fig. 2. Research flow diagram.

$$AE_k = -\sum_{i=1}^{12}\left(\frac{x_i}{\sum_{i=1}^{12} x_i}\right)\log_2\left(\frac{x_i}{\sum_{i=1}^{12} x_i}\right) \tag{3}$$

$$Change\ ratio = \frac{s \bullet n}{\overline{x}} \times 100 \tag{4}$$

where, x_i is the monthly value for ith month in kth year, s is the Sen's slope for annual AE, n is the number of years, and $\overline{x}$ is the average value in the study period.

AE quantifies how evenly hydroclimate variables are distributed across 12 months. Theoretically, AE values can range from zero to a maximum of $\log_2 12$ (≈ 3.585). High AE indicates a uniform distribution (low seasonality), while low AE suggests significant month-to-month differences (high seasonality). AE is useful for characterizing changes in a hydroclimatological context as it is statistically well-suited to the characteristics of precipitation, evaporation, and flow regimes (Mishra et al., 2009; Feng et al., 2013; Konapala et al., 2020; Wang et al., 2024).

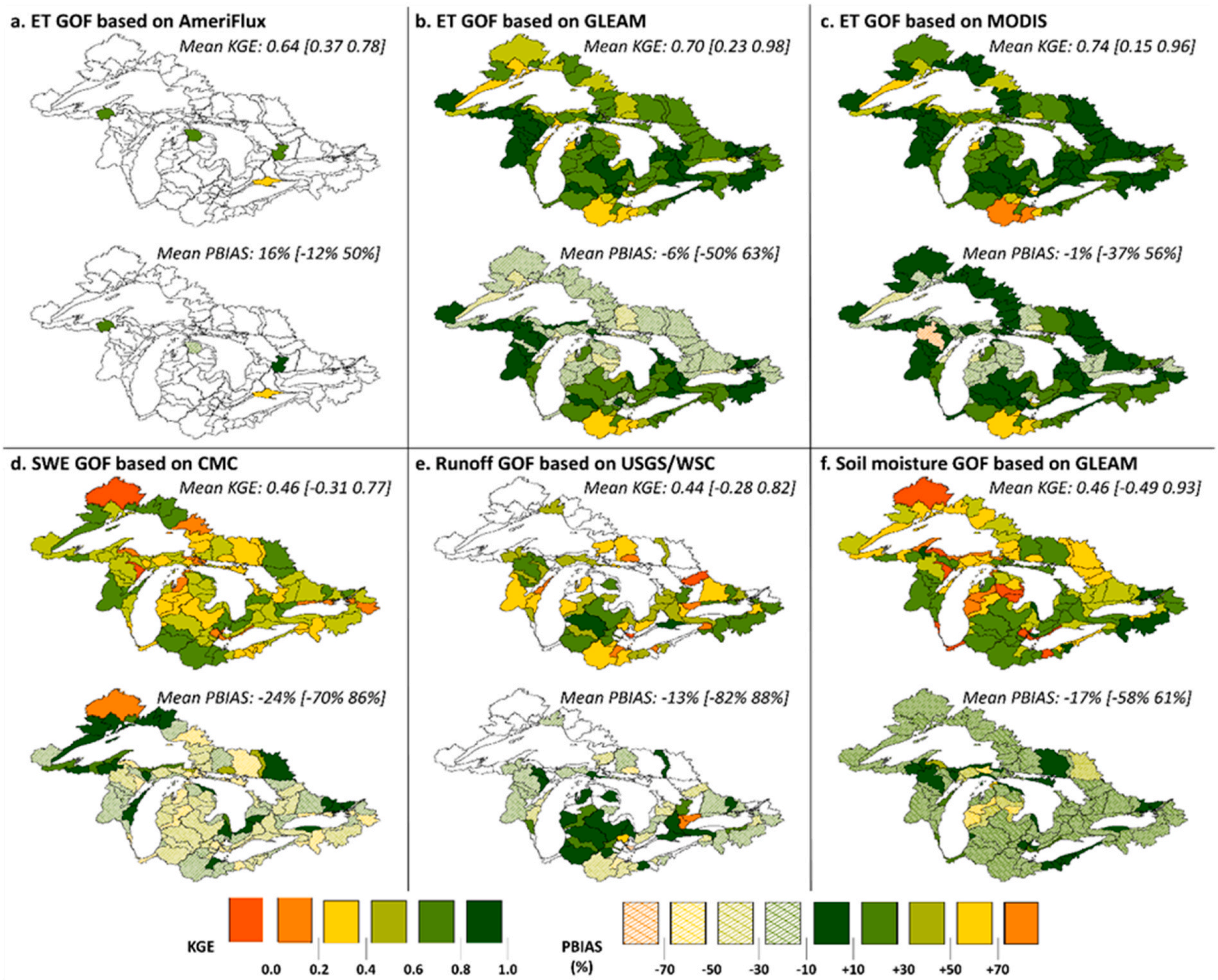

Fig. 3. Spatial distribution maps of Goodness-of-fit (GOF) statistics, including Kling-Gupta Efficiency (KGE) and Percentage Bias (PBIAS), for model evaluation using multiple reference datasets. Reference evapotranspiration (ET) datasets were obtained from AmeriFlux tower observations and two satellite-based products, the Global Land Evaporation Amsterdam Model (GLEAM) and the Moderate Resolution Imaging Spectroradiometer (MODIS). Reference datasets for snow water equivalent (SWE), runoff, and soil moisture were collected from the Canadian Meteorological Centre (CMC), the United States Geological Survey and Water Survey of Canada (USGS/WSC), and GLEAM, respectively. Subbasin-wide monthly averages were calculated for the period from 2001 to 2020.

3. Results

3.1. Evaluation of simulations against reference data

For the historical period from 2001 to 2020, the simulated hydrological components were evaluated by subbasin-wide monthly average values using various observations and satellite-based reference datasets (Fig. 3). In the case of ET evaluation, we have three reference datasets including in-situ measurements and two remote sensing-based modeling products (Table 1). For the Lake Erie subbasin, the simulated ET closely matches both satellite-based datasets, whereas it is greater than the in-situ flux tower dataset. The flux towers are located at the northeastern edge of the Lake Erie basin (Fig. 1), which is influenced by both land surface and lake effects, introducing noise into the in-situ measurements. This discrepancy has also been observed in a previous study (Fujisaki-Manome et al., 2017), which utilized other eddy covariance measurements from a location similar to our Ameriflux towers. For other subbasins, the simulated ET closely aligns with the in-situ dataset and mostly falls within observed ranges. Overall, simulated ET values have reasonable ranges compared to various reference datasets. The average KGE is greater than 0.6 and the average PBIAS is 16% for in-situ datasets and -6% and -1% for remote sensing products.

For other variables such as SWE, runoff, and surface soil moisture, there is a consistent pattern of underestimation across all basins. We found that WRF-Hydro encountered challenges in properly simulating albedo, which potentially influenced the underestimation of SWE, consequently affecting streamflow and surface soil moisture simulations (Figure S2). Despite this underestimation, the correlation coefficients for simulated hydrological variables, including SWE, runoff, and soil moisture, were high (e.g., 0.9 for all cases in Figure S2), demonstrating that the simulations could capture the overall patterns and long-term trends of the reference data. The average KGEs are greater than 0.4 and the average percentage biases are -24%, -13%, and -17% for SWE, runoff, and surface soil moisture, respectively. Since the primary objective of this study is to examine the changing patterns of long-term hydroclimate trends rather than determine absolute change magnitudes, model outputs can be used for further analysis. The potential sources of model bias are discussed in the Discussion section.

3.2. Analysis of annual trends and seasonality

3.2.1. Annual trends in hydroclimate components across basins

Fig. 4 illustrates the annual average magnitude of hydroclimate components for the four lake basins. Increasing trends are clearly observed in surface air temperature and ET, while SWE shows decreasing trends. Meanwhile, precipitation and runoff do not exhibit significant trends in their annual averages for the four lake basins. In addition, surface soil moisture shows increasing trends in the Erie and Ontario basins, whereas no significant trend is detected in the Michigan-Huron and Superior basins. Air temperature increases at a consistent rate of 0.02°C/year across all four lake basins, which have statistically significant trends. In contrast, statistically significant monotonic trends in precipitation are not detected, with large year-to-year variations observed. Substantial variations of the annual precipitation in the Great Lakes basin are also observed in previous studies (Hodgkins et al., 2007; Yang et al., 2023). Additional analyses of seasonal precipitation trends were conducted, but no significant changes were observed (Figure S3). Three lake basins, excluding Superior, show significant increases in annual ET. The Erie basin has the highest increase at 1.1 mm/year, followed by Ontario (0.7 mm/year) and Michigan-Huron (0.6 mm/year). The Superior basin, however, shows the smallest increase in ET at

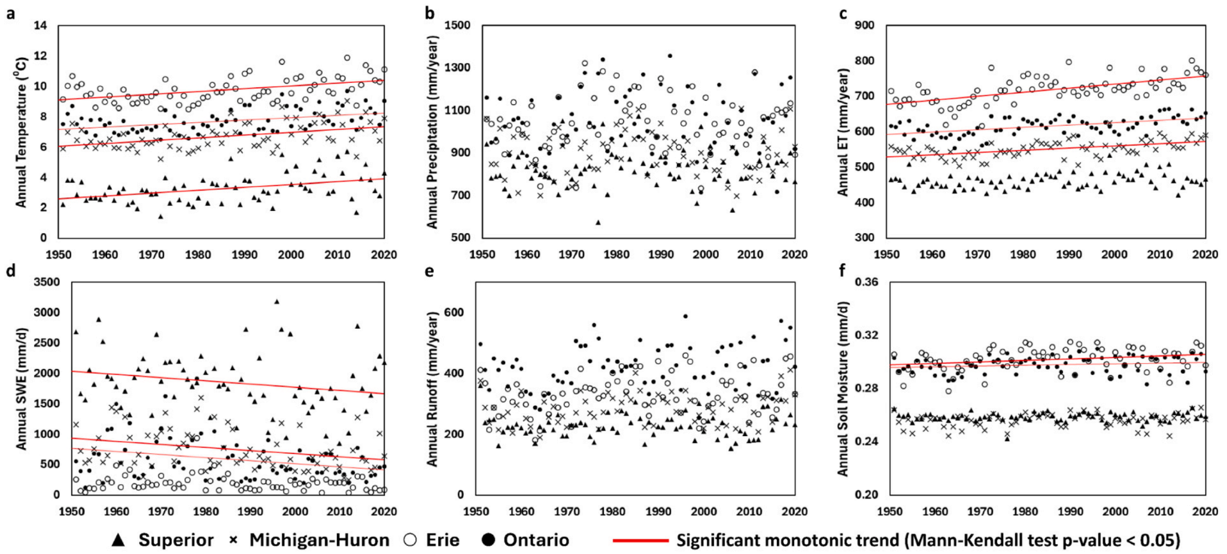

Fig. 4. Historical annual average hydroclimate variables (panels a through f) across each of the Great Lake basins (differentiated by symbols). Significant trends (per Mann-Kendall tests) are highlighted by a red line.

0.2 mm/year, which is not statistically significant. SWE trends are decreasing across all basins, with statistically significant decreases in three basins, excluding Erie.

The Superior basin shows the most substantial decrease in SWE at a rate of -6.1 mm/day, followed by Michigan-Huron (-4.6 mm/day), Ontario (-3.6 mm/day), and Erie (-0.8 mm/day). Trends in ET and SWE are strongly influenced by temperature trends rather than precipitation trends. This relationship is further explored in Section 3.4 using a correlation matrix between various hydroclimate variables. Runoff for all lake basins does not show a statistically significant trend (Fig. 4). The Great Lakes basin has distinct patterns of streamflow discharge due to the complex interactions of climate (e.g., precipitation and lake effect snowfall), groundwater, and surface runoff (Johnston and Shmagin, 2008). These interactions make it difficult to establish annual trends, resulting in non-monotonic annual patterns. Annual trends in surface soil moisture are statistically significant and increasing for the Erie and Ontario basins (both at 0.0001 mm/year), where soil moisture levels are considerably higher compared to the Michigan-Huron and Superior basins. The vegetation types in the northern and southern parts of the region are significantly different (Figure S1). The northern areas (e.g., the Michigan-Huron and Superior basins) are dominated by forests, while the southern areas (e.g., the Erie and Ontario basins) are dominated by cropland, which contributes to large differences in soil moisture between the two regions (Mao and Cherkauer, 2009). Overall, the Erie basin exhibits the most substantial changes in the annual magnitudes of hydroclimate components including temperature (0.018°C/year), precipitation (0.25 mm/year), ET (1.07 mm/year), and soil moisture (0.0001 mm/year). In contrast, the Superior basin shows the least changes in ET (0.24 mm/year), runoff (0.09 mm/year), and soil moisture (0.00001 mm/year), but the greatest decrease in SWE (-6.1 mm/year).

3.2.2. *Seasonal variations in hydroclimate components across basins*

Fig. 5 illustrates the monthly climatology of hydroclimate components for the four lake basins. SWE is considered only during the cold season (October to May). For air temperature, July and January are the warmest and coldest months, respectively, across all lake basins. The Superior basin experiences the largest seasonal differences (i.e., the differences between the highest and lowest months) with 32.7°C between 18.0°C (July) and -14.7°C (January) in the 1950s and 31.2°C in the 2000s, while the Erie basin has the smallest variation with 26.3°C between 21.9°C (July) and -4.4°C (April) in the 1950s and 26.1°C in the 2000s. In the case of precipitation, no consistent peak month was identified, although January to March typically represents the lowest precipitation for most basins. Again, the Superior basin shows the greatest seasonal differences, with values of 71.3 mm in the 1950s and 59.1 mm in the 2000s, while the Ontario and Erie basins have the least seasonal variations, with 27.2 mm and 33.4 mm in the 1950s and 2000s, respectively. Over time, seasonal differences in precipitation have decreased for most basins, except for the Ontario basin. For ET, July and January represent the highest and lowest months, similar to temperature. However, the Superior and Erie basins exhibit the smallest (72.6 mm in the 1950s and 71.7 mm in the 2000s) and largest (101.5 mm in the 1950s and 102.3 in the 2000s) seasonal differences, respectively, which is the opposite of the temperature pattern. These ET seasonal differences have remained relatively stable, with changes of less than 1 mm/month across all basins between the 1950s and 2000s.

SWE peaks in February or March and is at its lowest in October or May. The Superior basin shows the greatest monthly variations in SWE (330.9 cm in the 1950s and 264.8 cm in the 2000s), while the Erie basin shows the least (39.9 cm in the 1950s and 39.7 cm in the 2000s). Recently, the seasonal differences in SWE have decreased significantly in the Superior basin, with minimal changes observed in the Erie basin. Runoff generally peaks in April and reaches its lowest point in September for most basins. The Ontario basin displays the greatest seasonal differences in runoff (43.4 mm in the 1950s and 36.2 mm in the 2000s), while the Superior basin shows the least

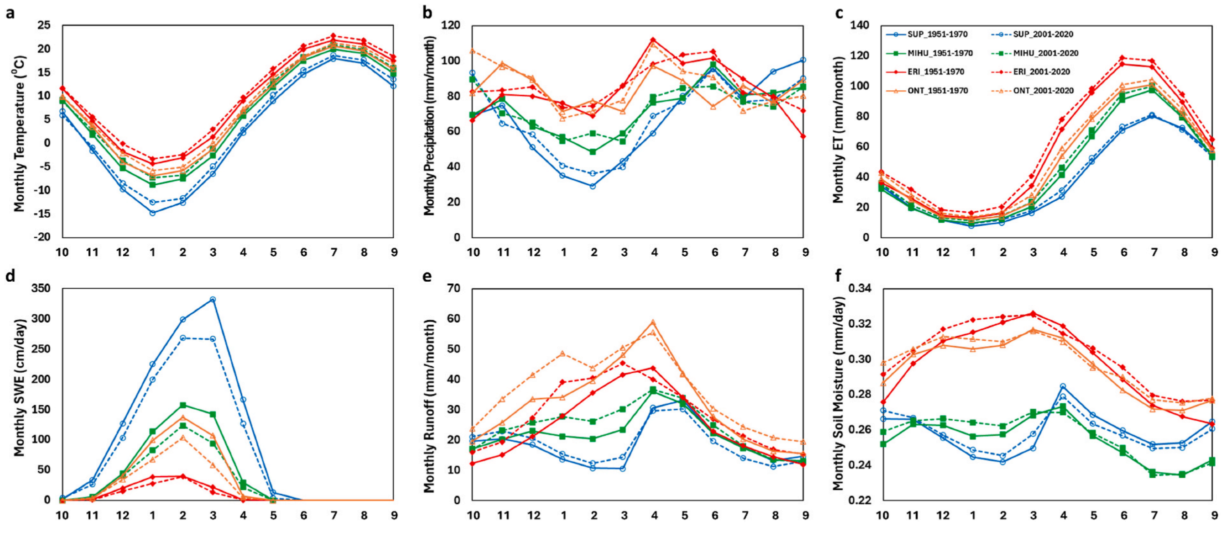

Fig. 5. Historical monthly average hydroclimate variables (panels a through e) across each of the Great Lakes basins (differentiated by colors and symbols: Superior (SUP), Michigan-Huron (MIHU), Erie (ERI), and Ontario (ONT)). Solid lines represent monthly averages from 1951 to 1970, and dotted lines represent monthly averages from 2001 to 2020.

(22.6 mm in the 1950s and 19.0 mm in the 2000s). Over time, seasonal differences in runoff have slightly declined across most basins. Lastly, soil moisture tends to peak in March or April and hits its lowest levels in August or September for most basins, except for the Superior basin, where February is the driest month. The Erie basin shows the greatest seasonal variation in soil moisture (0.06 mm in the 1950s and 0.05 mm in the 2000s), while the Superior basin shows the least (0.04 mm in the 1950s and 0.03 mm in the 2000s). Seasonal differences in soil moisture have generally decreased across all lake basins over time.

3.2.3. Changes in annual and seasonal trends

In the Great Lakes basin, most hydroclimate variables exhibit increased annual magnitudes and decreased seasonality between 1951–1970 and 2001–2020, except for precipitation and SWE (Fig. 6). Across all 121 subbasins, annual average air temperature is increasing monotonically with 95% confidence, with rates ranging from 0.13°C/year to 0.25°C/year. Higher rates are observed in the central and southern parts, including the western Michigan basin and the eastern Erie basin, while lower rates are observed in the northeastern parts of the region. Meanwhile, temperature seasonality generally decreases (Figure S4), though most changes are not statistically significant (only 4 out of 121 subbasins). Significant decreases are observed in the western parts of the region, including the Superior basin and the western Michigan basin. Although trends of precipitation magnitude increase in most areas (Figure S4), only one subbasin shows a statistically significant increase. There is no clear spatial pattern for the changes in annual precipitation magnitudes. Similarly, changing trends in precipitation seasonality vary, with some regions showing decreases and others increases (Figure S4). Only 10 out of 121 subbasins show statistically significant decreases in seasonality scattered throughout the region. There are no consistent trends in decreasing seasonality, but some of the eastern parts of the Superior and Michigan basins have increasing trends. Annual average ET increases at significant rates in most subbasins (117 out of 121) between 0.28 mm/year and 1.63 mm/year. The spatial trends of annual ET magnitude are similar to temperature, with relatively large increases in the southern parts of the region. In contrast, ET seasonality decreases in most regions, with 85 subbasins showing significant monotonic decreases, particularly in the northwestern areas including the Georgian Bay basin. Annual SWE decreases in all subbasins, with half (63 out of 121) showing statistically significant decreases ranging from −0.38 cm/day to −5.87 cm/day. Monthly variability of SWE increases in all subbasins (Figure S4), with 13 showing statistically significant increases, especially in the southern regions.

Annual runoff shows increasing trends in only 17 of 121 subbasins, with statistically significant trends ranging from 0.01 mm/year to 2.20 mm/year. The spatial pattern of changing trends in annual runoff is not clear, but there is a relatively large increase in the southern part of the region (or the southeastern Michigan basin). Runoff seasonality generally decreases over time, with 17 subbasins showing significant trends. The southern parts of the region show decreasing seasonality in runoff, while the northern parts of the Superior basin show increasing seasonality, but not statistically significant levels (Figure S4). Annual soil moisture shows statistically significant increases in 17 subbasins, with rates ranging from 0.0005 mm/year to 0.002 mm/year, showing relatively large increases in the southern region. Soil moisture seasonality increases in the central regions near the northern Michigan basin and decreases in the southern parts (Figure S4) with 23 subbasins identified as statistically significant levels of decreasing seasonality in soil moisture. The

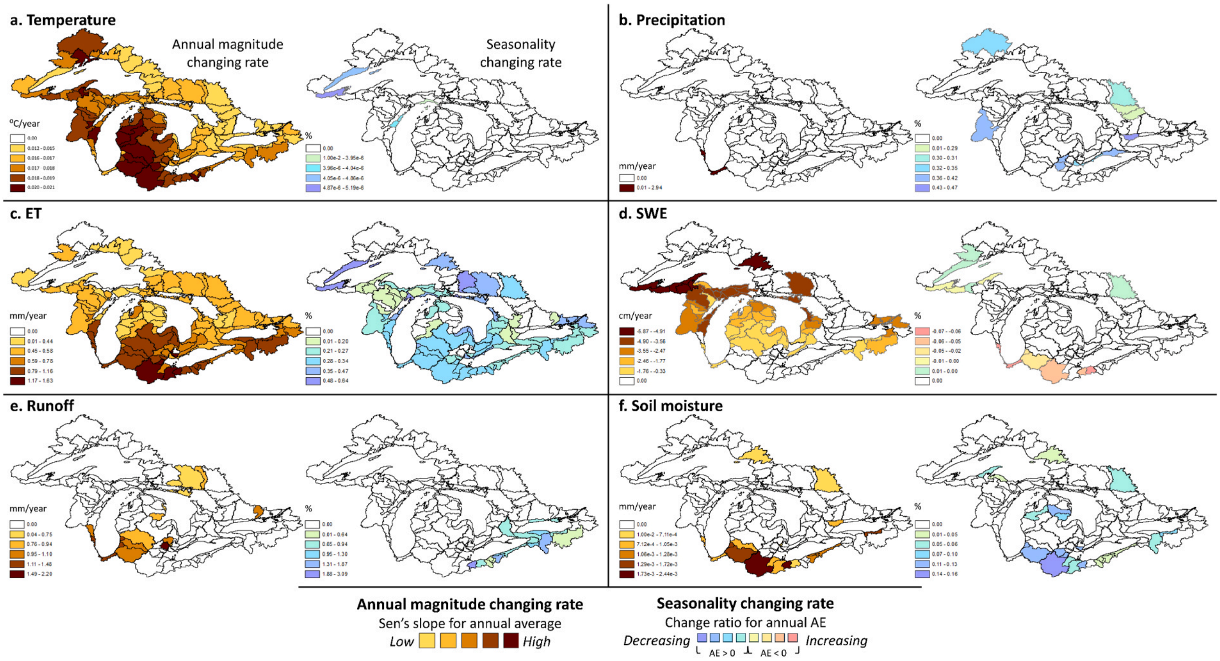

Fig. 6. Rate of change in annual and seasonal trends for hydroclimate variables from 1951 to 2020 across Great Lakes subbasins. Each panel shows the rate of change in annual magnitude (left side) and seasonality (right side) for each variable. Statistically significant trends are color-coded on a relative scale, with each panel having its own distinct numeric range.

southern part of the Great Lakes basin shows a general increase in the annual magnitude of soil moisture and a decrease in its seasonality. In contrast, the northern part, particularly the Michigan basin, exhibits a mild increase in the annual magnitude of soil moisture and a relatively large increase in its seasonality (Figure S4).

3.3. Comparison of multidecadal changes across hydroclimate components

Fig. 7 compares changes in various hydroclimate components between the recent two decades (2001–2020) and the earliest two decades of the study period (1951–1970). Air temperature, SWE, and runoff change more than other variables in terms of percentage changes of multidecadal averages, while precipitation, ET, and soil moisture show milder changes. The four lake basins generally exhibit consistent patterns of increase or decrease in these components, but some of them show regional differences. The mean air temperature has increased by 1°C on average for all lake basins over the most recent 20 years. The Superior basin shows the highest increase at 0.99°C (34% increase), followed by the Michigan-Huron basin at 0.95°C (15%), the Erie basin at 0.92°C (10%), and the Ontario basin at 0.80°C (10%). We counted the number of cold and warm days for 20 years (defined by the lowest and highest 10% of daily average temperatures) and calculated percentage change differences between the recent and past periods, which reveals an 18% decrease in cold days and a 26% increase in warm days on average. Mean annual precipitation has slightly increased by approximately 2%. To investigate the changes in extreme storm events, we first identified all rainfall events by grouping daily precipitation data into rainfall events that have consecutive rainy days (Song et al., 2020). Then, we calculated the intensity of each rainfall event (i.e., total rainfall depth/number of days). We set a threshold for extreme storm events as the top 10% of rainfall intensity among all rainfall events identified from 1951 to 2020 and counted the number of extreme storm events each year. The number of extreme rainfall events

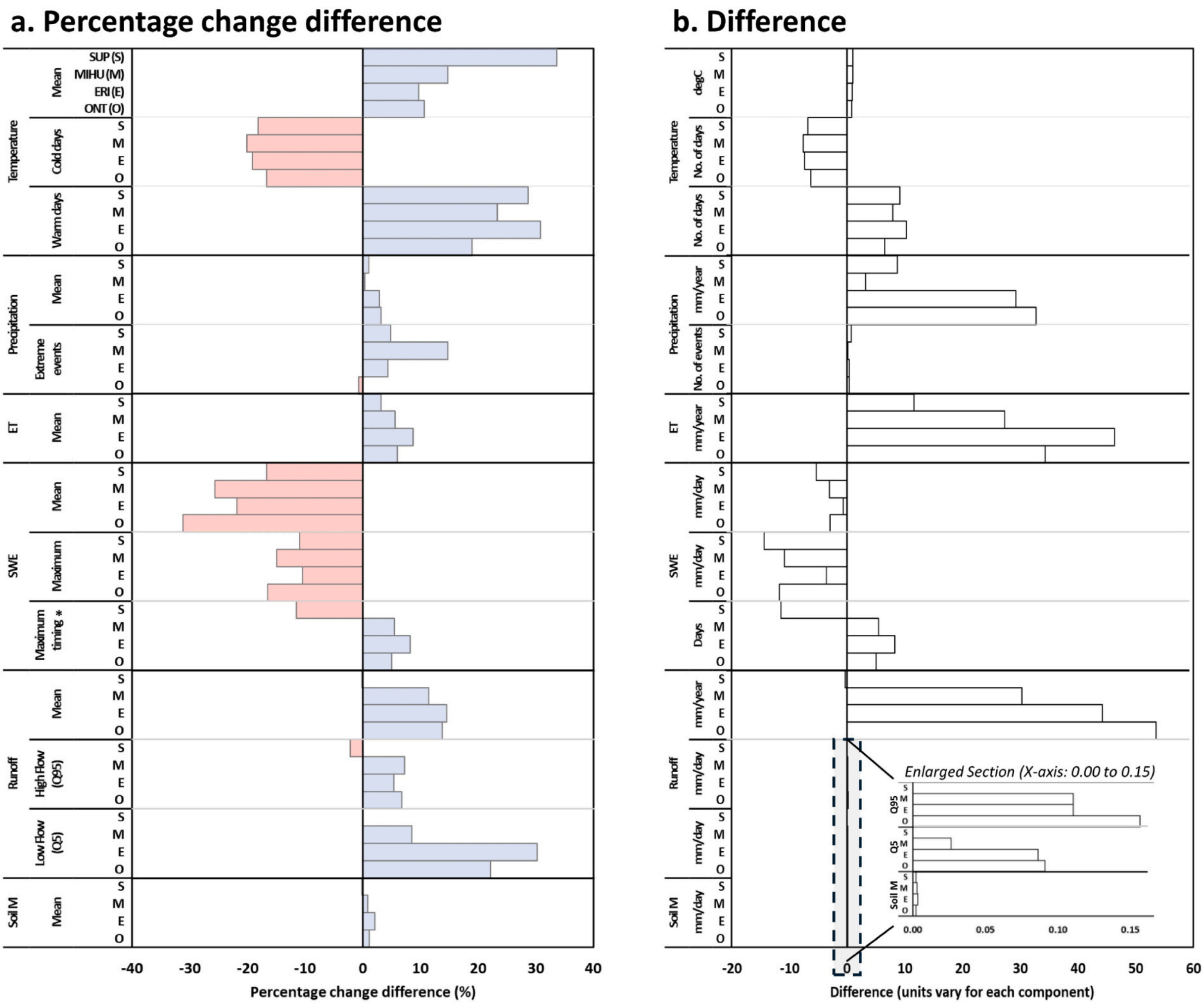

Fig. 7. Differences in average hydroclimate variables average between 2001–2020 and 1951–1970 for the Superior (S), Michigan-Huron (M), Erie (E), and Ontario (O) basins. Note * : Maximum SWE timing is represented as the difference in days between the two periods. For example, in the Erie basin, the maximum SWE timing shifted from February 7 (1951–1970) to February 15 (2001–2020), resulting in a difference of 8 days. Positive values indicate delayed maximum SWE timing, while negative values indicate earlier timing.

has increased for all lake basins except for the Ontario basin.

The annual ET across the four lake basins has increased by 6% on average. Notably, ET during the cold season (November to April) has risen by an average of 13%, while ET during the warm season by an average of 4% increase (not shown in the figure), which is consistent with Fig. 6 showing the reduction of ET seasonality over time. Both the mean annual and maximum SWE has decreased by 24% and 13%, respectively. The timing of maximum SWE has shifted, being delayed in three lake basins (e.g., from February 7 to February 15 in the Erie basin), while the Superior basin shows an earlier timing (from March 20 to March 9). For all lake basins excluding Superior, the annual average flow, high flow (95% of daily runoff), and low flow (5% of daily runoff) have increased by approximately 13%, 7%, and 20%, respectively. Meanwhile, the average and low flow in the Superior basin show less than 0% change and the high flow has decreased by about 2%. Except for the Superior basin, all three lake basins have substantial increases in flow. Surface soil moisture shows the least change, with less than a 2% increase across the four lake basins. Additionally, we observed that the southern basins, including the Erie and Ontario basins, show greater increases in soil moisture during the warm season than the cold season, but this was not the case for the northern basins (not shown in the figure).

3.4. Interrelationships between hydroclimate components

To investigate the annual and interannual relationships between various hydroclimate variables, we employed correlation coefficient matrices for annual, cold season, and warm season averages (Fig. 8 and Figure S5). This result underscores the importance of considering both seasonal and regional variations when assessing the impacts of climate change on hydroclimate dynamics in the Great Lakes basin. Air temperature shows strong positive correlations with ET (0.49 to 0.68) and strong negative correlations with SWE (-0.61 to -0.45) on an annual scale (Figure S5). This pattern holds for the cold season across all four lake basins. In the warm season, the temperature has positive correlations with ET and negative correlations with runoff and soil moisture, except for the Erie basin, which shows no significant correlations with most hydrological variables. In addition, the warm season temperature has negative correlations with cold season SWE in the northern basins (Superior and Michigan-Huron), but not significant correlations in the southern basins (Erie and Ontario). The results imply that cold season temperatures consistently impact ET and SWE for all lake basins, whereas warm season temperatures have varied regional impacts on hydrological processes. Precipitation exhibits strong positive correlations with runoff (0.59 to 0.72) and soil moisture (0.64 to 0.75) for all lake basins on an annual scale (Figure S5). In addition, it shows mild positive correlations with ET except for the Ontario basin. In both warm and cold seasons, strong positive correlations with runoff and soil moisture are identified for all basins. Additionally, positive correlations between precipitation and ET are observed in the warm season.

ET shows mild negative correlations with SWE (-0.42 to -0.25) across the four lake basins. On an annual scale, the correlations between ET and both runoff and soil moisture vary by basin: they are strong in the Erie basin, mild in the Ontario and Michigan-Huron

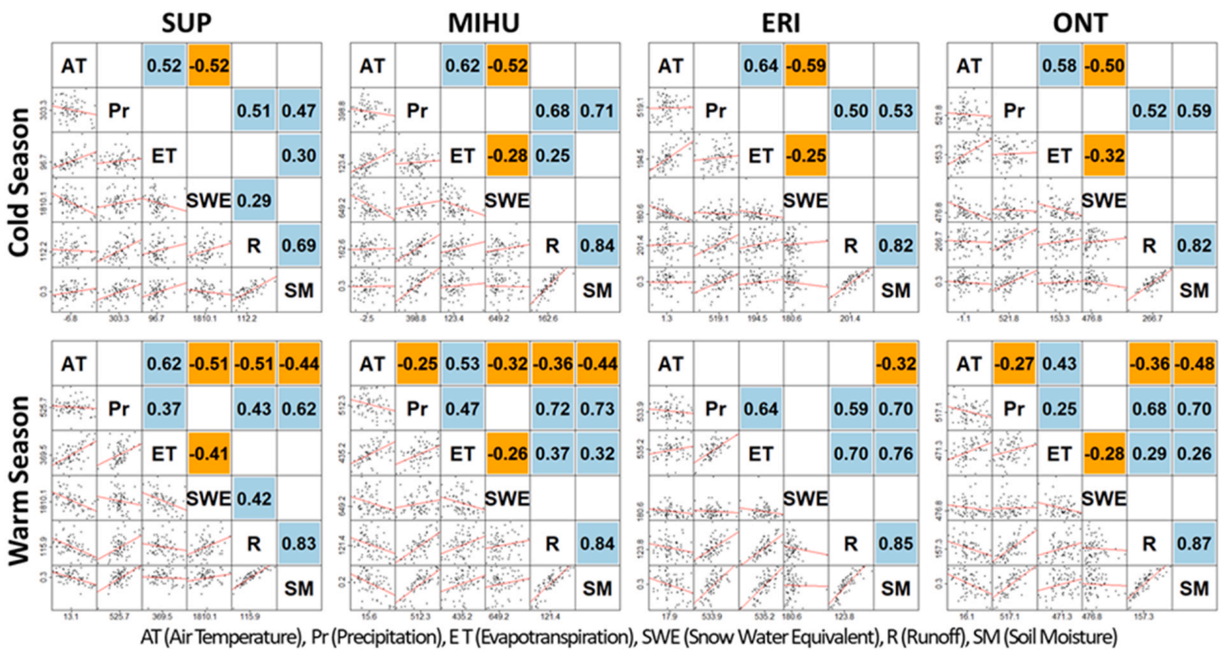

Fig. 8. Correlation among hydrological variables across cold and warm seasons for the four Great Lakes basins (Superior (SUP), Michigan-Huron (MIHU), Erie (ERI), and Ontario (ONT)). The lower-left of each subplot displays scatter plots with linear trendlines, while the upper-right shows statistically significant correlations (p-value < 0.05), highlighted with a blue and orange background, which shows positive and negative correlations, respectively. Note: SWE estimated during the cold season is used in the correlation analysis for the warm season to explore its interrelationships with warm season variables.

basins, and not significant in the Superior basin (Figure S5). In the cold season, ET maintains weak negative correlations with SWE for all basins but does not show significant correlations with runoff and soil moisture. In the warm season, ET has strong correlations with runoff and soil moisture in the Erie basin, while these correlations are mild in the Michigan-Huron and Ontario basins and nonexistent in the Superior basin. The negative correlations between ET and SWE indicate that temperature increases significantly drive increased ET and reduced SWE across all basins. SWE has a mild positive correlation with runoff for the Superior and Michigna-Huron basins on an annual scale (Figure S5). There are no significant correlations between either SWE and runoff or between SWE and soil moisture for both warm and cold seasons in all lake basins except for the Superior basin. Notably, in the Superior basin, SWE shows higher correlations with runoff in the warm season (0.42) than in the cold season (0.29). This implies that SWE significantly impacts runoff in the snow-dominated Superior basin for both warm and cold seasons, which is substantially different from the other basins. Runoff exhibits significant positive correlations with surface soil moisture across all basins during both warm and cold seasons. This indicates a close relationship between runoff and surface soil moisture levels. This result suggests that runoff and surface soil moisture are influenced by common driving factors including precipitation, temperature, and ET.

4. Discussion

4.1. Performance of hydrological simulations

We compared the performance of the hydrological simulation results with a previous model intercomparison study for the entire Great Lakes basin conducted by Mai et al. (2022) (see Table S1 in the Supplementary Materials). Since the model is primarily tuned for streamflow prediction during the 2008–2016 period (Cosgrove et al., 2024), the evaluation of other hydrological variables over the past 20 years highlights areas for improvement while also demonstrating the model's capacity to represent land surface and hydrological processes. The performance of runoff and SWE in this study is relatively lower than that of ET and soil moisture, which aligns with the accuracy observed in advanced models (or models with a similar level of complexity to WRF-Hydro) in Mai et al. (2022). According to the KGE criteria from Mai et al. (2022), simulated runoff, ET, SWE, and soil moisture show medium to good performance. Based on the PBIAS criteria (Mai et al., 2022), simulated ET using GLEAM and MODIS data is classified as excellent, while ET based on AmeriFlux is classified as good. Although the differences between these three reference datasets for ET are an interesting topic that has been widely explored in other studies (Wang et al., 2015; Khan et al., 2018; Zhang et al., 2020a; Zheng et al., 2022), this study focuses on long-term trends and overall model performance. Based on the comparisons with these datasets, we conclude that the simulated ET demonstrates good performance.

The simulated runoff and soil moisture meet the criteria for good performance as defined by PBIAS in Mai et al. (2022), while simulated SWE is classified between good and medium performance. We identified underestimations in simulated SWE, runoff, and soil moisture, with PBIAS values of −24 %, −13 %, and −17 %, respectively (Fig. 3). Given the significant role snow processes play in the hydrology of the Great Lakes basin, the underestimation of SWE affects the accuracy of simulated runoff and soil moisture. One possible reason for this underestimation is the inaccurate representation of snow processes in the model, which in turn affects snowmelt contributions to spring runoff and soil moisture (Shin et al., 2024). This study employed the calibrated parameter sets from NWMv2.1, which focused on tuning 14 model parameters to improve streamflow accuracy (Cosgrove et al., 2024). These parameters, related to soil, runoff, groundwater, vegetation, and snow processes, are crucial in WRF-Hydro, and studies have explored their sensitivities in modeling outputs (Yucel et al., 2015; Lahmers et al., 2019). However, only one parameter–specifically, the melt factor for the snow depletion curve–was considered for snow dynamics, which may contribute to the underestimation of modeling results in this study. Previous studies emphasize the importance of fine-tuning snow albedo schemes, such as optimizing snow depth, age, and minimum and maximum albedo, to enhance the accuracy of snow process simulations (Abolafia-Rosenzweig et al., 2022; Liu et al., 2022; Shin et al., 2024). Future studies should consider these factors to improve model performance. Another source of potential bias in the model results is the choice of input data, particularly the atmospheric forcing dataset, ERA5. This dataset differs from the one used for model calibration and contains biases compared to station-based observations (Table S2). ERA5 data is drier and warmer than station-based observations by 3.6 mm/year and 0.4°C, respectively, while the overall patterns are consistent (e.g., the average biases for monthly precipitation and temperature are -1% and 8% with corresponding average KGE values of 0.7 and 0.9) (Table S2). These biases likely contribute to the discrepancies in the simulation results.

To address the potential impacts of ERA5 on the hydrologic simulations, we compared the performance of the runoff simulations in this study with other studies using NWMv2.1, which incorporates AORC. Although detailed calibration and validation results (e.g., goodness-of-fit values) are not readily available, Cosgrove et al. (2024) reported that the median absolute bias for NWMv2.1 streamflow simulations is less than 20%, based on USGS streamflow datasets from approximately 10,000 stations across the United States for the period from 2013 to 2016. Additionally, Orendorf et al. (In Review, via personal communication) evaluated NWMv2.1 streamflow outputs for the period from 1979 to 2020, using a total of 157 USGS and WSC streamflow gauges across the Great Lakes basin, and found that the median KGE for the four lake basins (Superior, Michigan-Huron, Erie, and Ontario) ranged from 0.3 to 0.6. Despite differences in spatial and temporal coverage, these results are consistent with this study, where the median bias and KGE for runoff simulations are -16% and 0.5, respectively (Fig. 3). Given that NWMv2.1 is primarily designed for streamflow simulation, the evaluation of other hydrological outputs has been limited. These findings suggest that the level of accuracy in runoff simulations using ERA5 is comparable to that using AORC. We chose to use ERA5 due to its longer data period (available from 1940, compared to 1979 for AORC) and its well-documented reliability in the literature (AORC, by contrast, is a customized dataset specifically used for NWM calibration). However, ERA5 has high uncertainties during the earlier period (1950s to 1970s) due to the scarcity of in-situ datasets (Bell et al., 2021). In this study, we analyzed ERA5 air temperature and precipitation trends from 1960 to 2020 using station-based measurements and found that overall trends are in good agreement (Table S2). The updated version of ERA5 is currently in development to improve accuracy for early periods and is expected to be released in the near future (Bell et al., 2021). Future studies would benefit from incorporating these improvements into the land surface hydrological modeling.

4.2. Regional hot spots and spatial variability of hydroclimate trends

For the changes in annual magnitudes, the southern regions emerge as hotspots for increases in air temperature, ET, runoff, and soil moisture, while the northern regions are hotspots for decreases in SWE (Fig. 6). The significant increase in temperature across all subbasins, particularly in the central and southern parts, highlights the region's vulnerability to climate warming. In contrast, no hotspots were detected for precipitation, with only one subbasin showing a significant trend in annual precipitation magnitude. The absence of statistically significant precipitation changes in most subbasins underscores the complexity of precipitation patterns and their response to climate change in the Great Lakes region (Hayhoe et al., 2010; d'Orgeville et al., 2014; Zhang et al., 2020b). The widespread decrease in SWE, particularly in the northern regions, indicates a reduced snowpack, which may affect water availability during the melt season. The strong spatial correlation between temperature, ET, and SWE suggests that rising temperatures are driving higher ET rates and lower SWE rates, particularly in the southern regions. Regarding seasonality trends, most hydroclimate variables do not exhibit statistically significant changes, except for ET. In the case of ET, the northern parts of the region show relatively large decreases in seasonality compared to the southern parts. Temperature shows the least variation in seasonality among all hydroclimate variables. No consistent spatial trend is observed for precipitation seasonality. However, in the case of SWE, runoff, and soil moisture, a few subbasins in the southern regions show significant seasonality changes, with increases in SWE and decreases in runoff and soil moisture.

In the Great Lakes system, water flows from the northernmost, upstream region, the Superior basin, through the interconnected Michigan-Huron basin, eventually reaching the southern, downstream regions of the Erie and Ontario basins. Hydrological regimes differ substantially between these upstream and downstream areas, leading to distinct changing patterns in runoff and soil moisture (Fig. 7 and Figure S4). In the downstream region, rainfall-runoff relationships dominate, whereas in the upstream region, snow significantly influences runoff variability, soil moisture, and aquifer recharge (Grant et al., 2004; Maurer and Bowling, 2014). For instance, the upstream region exhibits decreasing runoff magnitude and increasing seasonality, while the downstream region shows the opposite. Similar trends are observed in soil moisture, showing increasing annual magnitudes and decreasing seasonality from upstream to downstream. These findings suggest that historical runoff and soil moisture trends are diverging between upstream and downstream regions, potentially influencing future hydrological patterns in the Great Lakes basin.

Overall, the Great Lakes basin is undergoing significant shifts in hydroclimate variables, including notable increases in temperature and ET and decreases in SWE. These changes are not uniform across the basin, a trend consistent with findings from studies across the world (Feng et al., 2013; Vano et al., 2015; Konapala et al., 2020; Wang et al., 2023). Konapala et al. (2020) project that the Great Lakes region, characterized by high precipitation and low seasonality regime, will experience increased annual magnitude of evaporation with decreased seasonality, which aligns with our results. However, Konapala et al. (2020) also found that precipitation is projected to increase both annual magnitude and seasonality, while these patterns were not evident in our long-term historical trends analysis. Both historical and future ET trends show a clear and consistent direction, unlike the more variable precipitation trends. This discrepancy is likely stemming from the substantial uncertainties in precipitation estimates across global climate models (Song et al., 2020). The distinct spatial patterns in both magnitude and seasonality emphasize the need for region-specific studies and adaptive management strategies (e.g., a series of regional studies about the Great Lakes basin; Fry et al., 2014; Gaborit et al., 2017; Mai et al., 2021; 2022).

4.3. Drivers of hydroclimate trends

The analysis of multidecadal hydroclimate trends in the Great Lakes basin reveals a complex and interconnected system, where changes in air temperature, precipitation, ET, SWE, runoff, and soil moisture are driven by regional climate dynamics. These trends not only highlight shifts in individual hydroclimate components but also illustrate how these components interact and influence one another. Understanding the magnitude and variability of these trends, as well as their broader implications, is critical for developing adaptive strategies for water management, ecosystem conservation, and climate resilience both within the Great Lakes basin and in other regions with similar climatic conditions.

Surface air temperature trends have exhibited the most significant changes across the Great Lakes basin, with more rapid warming observed in the last two decades (2001–2020) compared to the 1950s (1951–1970) (Fig. 7). These air temperature trends closely align with long-term trends in lake surface water temperature over a similar period (1979–2021), showing significant increases of 0.4°C to 0.6°C per decade, which are consistent with our findings (Cannon et al., 2024). The increase in warm days and the decrease in cold days highlight the region's vulnerability to climate warming. These temperature-driven changes are driving shifts in hydrologic processes, particularly influencing ET and SWE throughout the year, while runoff and soil moisture primarily during the warm season (Fig. 8). Warmer temperatures increase atmospheric moisture demand, leading to higher ET rates, which, in turn, reduce soil moisture and limit runoff generation. This effect is especially pronounced in the warm season when increased evaporative losses deplete surface and subsurface water storage, amplifying seasonal drought risk and altering the timing and magnitude of streamflow. During the cold season, rising temperatures negatively impact SWE by reducing snow accumulation and accelerating melt processes. In the northern basins, temperatures in the warm season are further linked to reduced cold season SWE, potentially due to delayed snowfall onset, increased rain-on-snow events, and alterations in soil freeze-thaw dynamics (Rixen et al., 2022).

While annual precipitation has only slightly increased across the region, the frequency and intensity of extreme rainfall events have increased, especially during the fall and winter seasons (Figure S3). This pattern suggests that while the total amount of precipitation remains relatively stable, its distribution and intensity are shifting. Extreme storm events, particularly in the southern basins, pose a growing risk to infrastructure and water management systems. These findings align with broader trends of increasing extreme weather events globally (Hayhoe et al., 2010; d'Orgeville et al., 2014).

4.4. Interrelationships between hydrologic processes

ET has increased across the Great Lakes basin, with a more pronounced increase during the cold season (Fig. 7). The relatively strong correlation between temperature and ET, particularly during the cold season (Fig. 8), emphasizes the role of temperature as a key driver of changes in ET, which is discussed in the previous section. Although the increase in ET is smaller than the percentage increase in temperature, it exceeds the changes in precipitation, suggesting that temperature will have a more significant influence on ET on a multidecadal scale. However, ET is not solely influenced by temperature; it is also affected by factors such as solar radiation, humidity, and wind speed (Lofgren et al., 2011).

SWE has decreased significantly across the basin, with the timing of maximum SWE shifting in all lake basins. The Superior basin, in particular, shows an earlier melt of snowpack, while other basins show delayed snowmelt. The declining snowpack is a clear signal of climate change impact on cold season hydrology, as warmer winters reduce snow accumulation and shift the timing of snowmelt. The reduction in snowpack and altered timing of snowmelt have direct consequences for spring runoff and water availability during the growing season. Regions dependent on snowmelt for water supplies, including agricultural and urban areas, may face water shortages as the timing and volume of snowmelt change. This trend is particularly concerning for other cold regions, such as the Himalayas (Maurer et al., 2019), the Alps (Carrer et al., 2023), and the Rocky Mountains (Wieder et al., 2022), where declining snowpack can disrupt water supplies for billions of people.

Runoff has increased in all basins except the Superior basin, where little to no change was observed. The Superior basin, with its colder climate and prolonged ice cover, experiences later snowmelt compared to the southern basins due to delayed warming and insulation from the ice, leading to less runoff variability compared to basins with warmer climates (Fig. 5e). Higher high-flow events increase flood risks, while increased low-flow events can exacerbate droughts. Regions with similar rainfall and snow dynamics may experience similar shifts in runoff patterns, calling for more adaptive water management strategies that account for increased variability in flow regimes.

Of all the hydroclimate variables analyzed, soil moisture exhibits the least change across the four lake basins. This suggests that surface soil moisture is less sensitive to climatic changes compared to other hydroclimate variables, which is also observed in Mao and Cherkauer (2009). The relative stability of soil moisture reflects the complex interactions between precipitation, temperature, and land use. However, regional differences exist, with southern basins showing greater increases in soil moisture during the warm season compared to northern basins. This result is aligned with a previous study (Erler et al., 2019), which investigated the main driver of seasonal soil moisture changes in the southern part of the Great Lakes basin. Soil moisture is a critical factor for agriculture and ecosystem health, and even small changes could have cascading effects on land use and water availability. While soil moisture has remained relatively stable, localized changes in precipitation patterns, land use, and temperature could lead to more variability in the future.

The trends observed in the Great Lakes basin may manifest in other areas with similar hydroclimate dynamics, such as temperate and polar regions across the globe. The interplay between warming temperatures, changing precipitation patterns, and declining snowpack is likely to affect water availability, flood risk, and ecosystem dynamics in these regions. For instance, the decreasing snowpack and altered runoff timing in the Great Lakes basin mirror trends observed in the European Alps, the Rocky Mountains, and the Himalayas, where similar hydroclimate challenges are emerging (Maurer et al., 2019; Wieder et al., 2022; Carrer et al., 2023). As extreme weather events, including intense rainfall and heatwaves, become more frequent worldwide, regions will need to adapt their infrastructure and water management practices to handle increased variability. This includes redesigning flood control measures, investing in irrigation efficiency, and developing strategies to cope with earlier snowmelt and reduced water availability during critical growing seasons.

5. Conclusions

This study comprehensively analyzes the long-term hydroclimate changes across the Great Lakes basin from 1951 to 2020. Overall, the Great Lakes basin is undergoing significant shifts in hydroclimate variables; notable increases in air temperature, ET, and runoff (particularly low flow), and decreases in SWE. Significant spatial and temporal variations are also identified within the region. In the northernmost region, the Superior basin, runoff, and soil moisture exhibit decreasing magnitude with increasing seasonality, whereas the southern regions (Erie and Ontario basins) display the opposite trend. Notably, the Erie basin showed the most substantial changes in annual magnitude for hydroclimate components, albeit with only minor shifts in seasonality, while the Superior basin experienced minor changes in annual magnitude but the most pronounced decrease in SWE.

This study acknowledges factors that may influence the results, including biases in the early period of the reanalysis dataset and challenges in accurately representing the snow process in the land surface model. Extensive evaluations were conducted using various references such as in-situ measurements, satellite-based products, and literature. Though the overall patterns in the input data and model outputs demonstrate good agreement with these references supporting their use for long-term trend analysis, the inherent uncertainties could influence the results. Therefore, we recommend that future studies utilize updated reanalysis datasets and further refine the land surface modeling schemes.

The findings of this study emphasize the need for region-specific studies and adaptive management approaches when assessing the impacts of climate change on hydroclimate dynamics. This long-term analysis of hydroclimate trends provides valuable references for understanding historical changes and offers critical implications for future conditions. These insights highlight the complexity and regional variability of hydroclimate interactions in the Great Lakes basin, emphasizing the need for localized studies and tailored management approaches.

CRediT authorship contribution statement

Fujisaki-Manome Ayumi: Writing – review & editing, Methodology, Conceptualization. **Cannon David:** Writing – review & editing, Methodology, Conceptualization. **Hong Yi:** Writing – review & editing, Methodology, Conceptualization. **Fry Lauren M.:** Writing – review & editing, Methodology, Conceptualization. **Gronewold Andrew D.:** Writing – review & editing, Resources, Methodology, Funding acquisition, Conceptualization. **Shin Satbyeol:** Writing – review & editing, Writing – original draft, Visualization, Validation, Software, Methodology, Investigation, Formal analysis, Data curation, Conceptualization.

Declaration of Generative AI and AI-assisted technologies in the writing process

During the preparation of this work, the author(s) used ChatGPT in order to improve the readability and language of the work. After using this tool/service, the author(s) reviewed and edited the content as needed and take(s) full responsibility for the content of the publication.

Declaration of Competing Interest

The authors declare that they have no known competing financial interests or personal relationships that could have appeared to influence the work reported in this paper.

Acknowledgments

We appreciate Sophie Orendorf for her support in retrieving streamflow datasets from USGS and WSC online platforms across the Great Lakes basin. This work was supported by the Framework for Resilient Great Lakes Restoration Initiative (GLRI) Investments Project through a collaborative partnership between the Cooperative Institute for Great Lakes Research (CIGLR), the National Oceanic and Atmospheric Administration (NOAA), the United States Army Corps of Engineers (USACE), and the United States Geological Survey (USGS). Funding was awarded to CIGLR through the NOAA Cooperative Agreement with the University of Michigan (CIGLR Award No. NA22OAR4320150). This is CIGLR contribution 1261 and NOAA Great Lakes Environmental Research Laboratory (GLERL) Contribution 2075. ADG was also supported through the NSF Global Centers program (NSF Award No. 2330317).

Appendix A. Supporting information

Supplementary data associated with this article can be found in the online version at doi:10.1016/j.ejrh.2025.102347.

Data Availability

Data will be made available on request. The ERA5 data were obtained from the Copernicus Climate Change Service (https://cds.climate.copernicus.eu). The list of the land surface datasets used in NWMv2.1 can be found in the Noah-Multiparameterization Land Surface Model document (https://ral.ucar.edu/model/noah-multiparameterization-land-surface-model-noah-mp-lsm), The hydrographic data for the United States portion was obtained from the National Hydrography Dataset Plus version 2 (NHDPlus v2) provided by the United States Geological Survey (USGS; https://nhdplus.com/NHDPlus/), and that for the Canadian portion was obtained from the Great Lakes hydrography data set (GLHD; https://www.glahf.org/watersheds/). The land use for the United States portion was obtained from the National Land Cover Database (NLCD) produced by USGS (https://www.mrlc.gov/), and that for the Canadian portion (Ontario province) was obtained from the modified Moderate Resolution Imaging Spectroradiometer (MODIS /) dataset produced by Boston University (https://www.umb.edu/spectralmass/terra-aqua-modis/). The soil data for the United States portion was obtained from the State Soil Geographic Database (STATSGO) database produced by the United States Department of Agriculture (USDA) (http://websoilsurvey.nrcs.usda.gov/) and that for the Canadian portion was obtained from the Food and Agriculture Organization (FAO) Soil Map of the World (FAO/UNESCO 1971). The WRF-Hydro modeling outputs can be downloaded in the University of Michigan - Deep Blue Data (https://doi.org/10.7302/wkd1-nb64).

References

Abolafia-Rosenzweig, R., He, C., McKenzie Skiles, S., Chen, F., Gochis, D., 2022. Evaluation and optimization of snow albedo scheme in Noah-MP land surface model using in situ spectral observations in the Colorado Rockies.), pp. e2022MS003141 J. Adv. Model. Earth Syst. 14 (10). https://doi.org/10.1029/2022MS003141.

Adnan, R.M., Mirboluki, A., Mehraein, M., Malik, A., Heddam, S., Kisi, O., 2024. Improved prediction of monthly streamflow in a mountainous region by metaheuristic-enhanced deep learning and machine learning models using hydroclimatic data. Theor. Appl. Climatol. 155 (1), 205–228. https://doi.org/10.1007/s00704-023-04624-9.

Althoff, D., Rodrigues, L.N., 2021. Goodness-of-fit criteria for hydrological models: Model calibration and performance assessment. J. Hydrol. 600, 126674. https://doi.org/10.1016/j.jhydrol.2021.126674.

Arain, A. 2018a. AmeriFlux BASE CA-TP1 Ontario - Turkey Point 2002 Plantation White Pine, Ver. 3-5, AmeriFlux AMP, (Dataset). https://doi.org/10.17190/AMF/1246009.

Arain, A. 2018b. AmeriFlux BASE CA-TP3 Ontario - Turkey Point 1974 Plantation White Pine, Ver. 3-5, AmeriFlux AMP, (Dataset). https://doi.org/10.17190/AMF/1246011.

Arain, A. 2018c. AmeriFlux BASE CA-TP4 Ontario - Turkey Point 1939 Plantation White Pine, Ver. 4-5, AmeriFlux AMP, (Dataset). https://doi.org/10.17190/AMF/1246012.

Arain, A. 2018d. AmeriFlux BASE CA-TPD Ontario - Turkey Point Mature Deciduous, Ver. 2-5, AmeriFlux AMP, (Dataset). https://doi.org/10.17190/AMF/1246152.

Balsamo, G., Agusti-Parareda, A., Albergel, C., Arduini, G., Beljaars, A., Bidlot, J., Blyth, E., Bousserez, N., Boussetta, S., Brown, A., Buizza, R., 2018. Satellite and in situ observations for advancing global Earth surface modelling: a review. Remote Sens. 10 (12), 2038. https://doi.org/10.3390/rs10122038.

Bell, B., Hersbach, H., Simmons, A., Berrisford, P., Dahlgren, P., Horányi, A., Muñoz-Sabater, J., Nicolas, J., Radu, R., Schepers, D., Soci, C., 2021. The ERA5 global reanalysis: preliminary extension to 1950. Q. J. R. Meteorol. Soc. 147 (741), 4186–4227. https://doi.org/10.1002/qj.4174.

Bierkens, M.F., Bell, V.A., Burek, P., Chaney, N., Condon, L.E., David, C.H., Roo, A., Döll, P., Drost, N., Famiglietti, J.S., Flörke, M., 2015. Hyper-resolution global hydrological modelling: what is next? Hydrol. Process. 29 (2). https://doi.org/10.1002/hyp.10391.

Brown, R.D. and B. Brasnett. 2010. Canadian Meteorological Centre (CMC) Daily Snow Depth Analysis Data, Version 1. NASA National Snow and Ice Data Center Distributed Active Archive Center. Boulder, Colorado USA. https://doi.org/10.5067/W9FOYWH0EQZ3.

Byun, K., Chiu, C.M., Hamlet, A.F., 2019. Effects of 21st century climate change on seasonal flow regimes and hydrologic extremes over the Midwest and Great Lakes region of the US. Sci. Total Environ. 650, 1261–1277. https://doi.org/10.1016/j.scitotenv.2018.09.063.

Cai, X., Yang, Z.L., David, C.H., Niu, G.Y., Rodell, M., 2014. Hydrological evaluation of the Noah-MP land surface model for the Mississippi River Basin. J. Geophys. Res.: Atmospheres 119 (1), 23–38. https://doi.org/10.1002/2013JD020792.

Cannon, D., Wang, J., Fujisaki-Manome, A., Kessler, J., Ruberg, S., Constant, S., 2024. Investigating multidecadal trends in ice cover and subsurface temperatures in the laurentian great lakes using a coupled hydrodynamic–ice model. J. Clim. 37 (4), 1249–1276. https://doi.org/10.1175/JCLI-D-23-0092.1.

Carrer, M., Dibona, R., Prendin, A.L., Brunetti, M., 2023. Recent waning snowpack in the Alps is unprecedented in the last six centuries. Nat. Clim. Change 13 (2), 155–160. https://doi.org/10.1038/s41558-022-01575-3.

Chen, H., Guo, S., Xu, C.Y., Singh, V.P., 2007. Historical temporal trends of hydro-climatic variables and runoff response to climate variability and their relevance in water resource management in the Hanjiang basin. J. Hydrol. 344 (3-4), 171–184. https://doi.org/10.1016/j.jhydrol.2007.06.034.

Clark, M.P., Fan, Y., Lawrence, D.M., Adam, J.C., Bolster, D., Gochis, D.J., Hooper, R.P., Kumar, M., Leung, L.R., Mackay, D.S., Maxwell, R.M., 2015. Improving the representation of hydrologic processes in Earth System Models. Water Resour. Res. 51 (8), 5929–5956. https://doi.org/10.1002/2015WR017096.

Cosgrove, B., Gochis, D., Flowers, T., Dugger, A., Ogden, F., Graziano, T., Clark, E., Cabell, R., Casiday, N., Cui, Z., Eicher, K., 2024. NOAA's national water model: advancing operational hydrology through continental-scale modeling. J. Am. Water Resour. Assoc. 60, 247–272. https://doi.org/10.1111/1752-1688.13184.

Croley, T., 2002. Large basin runoff model. Chapter 17. In: Singh, V., Frevert, D., Meyer, S. (Eds.), Mathematical Models of Large Watershed Hydrology. Water Resources Publications, CO, USA, pp. 717–770.

Desai, A. 2023. AmeriFlux BASE US-Syv Sylvania Wilderness Area, Ver. 26-5, AmeriFlux AMP, (Dataset). https://doi.org/10.17190/AMF/1246106.

Dong, C., 2018. Remote sensing, hydrological modeling and in situ observations in snow cover research: A review. J. Hydrol. 561, 573–583. https://doi.org/10.1016/j.jhydrol.2018.04.027.

d'Orgeville, M., Peltier, W.R., Erler, A.R., Gula, J., 2014. Climate change impacts on Great Lakes Basin precipitation extremes. J. Geophys. Res.: Atmos. 119 (18), 10–799. https://doi.org/10.1002/2014JD021855.

Duan, Y., Kumar, S., 2020. Predictability of seasonal streamflow and soil moisture in national water model and a humid Alabama–Coosa–Tallapoosa River basin. J. Hydrometeorol. 21 (7), 1447–1467. https://doi.org/10.1175/JHM-D-19-0206.1.

Ek, M.B., Mitchell, K.E., Lin, Y., Rogers, E., Grunmann, P., Koren, V., Gayno, G., Tarpley, J.D., 2003. Implementation of Noah land surface model advances in the National Centers for Environmental Prediction operational mesoscale Eta model. J. Geophys. Res.: Atmos. 108 (D22). https://doi.org/10.1029/2002JD003296.

Erler, A.R., Frey, S.K., Khader, O., d'Orgeville, M., Park, Y.J., Hwang, H.T., Lapen, D.R., Peltier, W.R., Sudicky, E.A., 2019. Evaluating climate change impacts on soil moisture and groundwater resources within a lake-affected region. Water Resour. Res. 55 (10), 8142–8163. https://doi.org/10.1029/2018WR023822.

Fall, G., Kitzmiller, D., Pavlovic, S., Zhang, Z., Patrick, N., St. Laurent, M., Trypaluk, C., Wu, W., Miller, D., 2023. The office of water prediction's analysis of record for calibration, version 1.1: dataset description and precipitation evaluation. JAWRA J. Am. Water Resour. Assoc. 59 (6), 1246–1272. https://doi.org/10.1111/1752-1688.13143.

Fatichi, S., Vivoni, E.R., Ogden, F.L., Ivanov, V.Y., Mirus, B., Gochis, D., Downer, C.W., Camporese, M., Davison, J.H., Ebel, B., Jones, N., 2016. An overview of current applications, challenges, and future trends in distributed process-based models in hydrology. J. Hydrol. 537, 45–60. https://doi.org/10.1016/j.jhydrol.2016.03.026.

Feng, X., Porporato, A., Rodriguez-Iturbe, I., 2013. Changes in rainfall seasonality in the tropics. Nat. Clim. Change 3 (9), 811–815. https://doi.org/10.1038/nclimate1907.

Fry, L.M., Gronewold, A.D., Fortin, V., Buan, S., Clites, A.H., Luukkonen, C., Holtschlag, D., Diamond, L., Hunter, T., Seglenieks, F., Durnford, D., 2014. The great lakes runoff intercomparison project phase 1: Lake Michigan (GRIP-M). J. Hydrol. 519, 3448–3465. https://doi.org/10.1016/j.jhydrol.2014.07.021.

Fujisaki-Manome, A., Fitzpatrick, L.E., Gronewold, A.D., Anderson, E.J., Lofgren, B.M., Spence, C., Chen, J., Shao, C., Wright, D.M., Xiao, C., 2017. Turbulent heat fluxes during an extreme lake-effect snow event. J. Hydrometeorol. 18 (12), 3145–3163. https://doi.org/10.1175/JHM-D-17-0062.1.

Gaborit, É ., Fortin, V., Tolson, B., Fry, L., Hunter, T., Gronewold, A.D., 2017. Great Lakes runoff inter-comparison project, phase 2: Lake Ontario (GRIP-O). J. Gt. Lakes Res. 43 (2), 217–227. https://doi.org/10.1016/j.jglr.2016.10.004.

Gesch, D., Oimoen, M., Greenlee, S., Nelson, C., Steuck, M., Tyler, D., 2002. The national elevation dataset. Photogramm. Eng. Remote Sens. 68 (1), 5–11.

Gochis, D.J., Barlage, M., Dugger, A., FitzGerald, K., Karsten, L., McAllister, M., McCreight, J., Mills, J., RafieeiNasab, A., Read, L. and Sampson, K., 2020. The WRF-Hydro modeling system technical description (Version 5.2). University Corporation for Atmospheric Research: Boulder, CO, USA.

Gough, C., Bohrer, G., Curtis, P., 2023a. AmeriFlux AMP, (Dataset). Am. BASE US-UMB Univ. Mich. Biol. Station Ver. 19–5. https://doi.org/10.17190/AMF/1246107.

Gough, C., Bohrer, G., Curtis, P., 2023b. AmeriFlux BASE US-UMd UMBS Disturbance, Ver. 14-5, AmeriFlux AMP, (Dataset). https://doi.org/10.17190/AMF/1246134.

Grant, L., Seyfried, M., McNamara, J., 2004. Spatial variation and temporal stability of soil water in a snow-dominated, mountain catchment. Hydrol. Process. 18 (18), 3493–3511. https://doi.org/10.1002/hyp.5798.

Gronewold, A.D., Clites, A.H., Hunter, T.S., Stow, C.A., 2011. An appraisal of the Great Lakes advanced hydrologic prediction system. J. Gt. Lakes Res. 37 (3), 577–583. https://doi.org/10.1016/j.jglr.2011.06.010.

Gronewold, A.D., Fortin, V., 2012. Advancing Great Lakes hydrological science through targeted binational collaborative research. Bull. Am. Meteorol. Soc. 93 (12), 1921–1925. https://doi.org/10.1175/BAMS-D-12-00006.1.

Gronewold, A.D., Fortin, V., Lofgren, B., Clites, A., Stow, C.A., Quinn, F., 2013. Coasts, water levels, and climate change: a great Lakes perspective. Clim. Change 120, 697–711. https://doi.org/10.1007/s10584-013-0840-2.

Gupta, H.V., Kling, H., Yilmaz, K.K., Martinez, G.F., 2009. Decomposition of the mean squared error and NSE performance criteria: implications for improving hydrological modelling. J. Hydrol. 377 (1-2), 80–91. https://doi.org/10.1016/j.jhydrol.2009.08.003.

Hayhoe, K., VanDorn, J., Croley, I.I., T., Schlegal, N., Wuebbles, D., 2010. Regional climate change projections for Chicago and the US Great Lakes. J. Gt. Lakes Res. 36, 7–21. https://doi.org/10.1016/j.jglr.2010.03.012.

He, C., Valayamkunnath, P., Barlage, M., Chen, F., Gochis, D., Cabell, R., Schneider, T., Rasmussen, R., Niu, G.Y., Yang, Z.L., Niyogi, D., 2023. Modernizing the open-source community Noah with multi-parameterization options (Noah-MP) land surface model (version 5.0) with enhanced modularity, interoperability, and applicability. Geosci. Model Dev. 16 (17), 5131–5151. https://doi.org/10.5194/gmd-16-5131-2023.

Hersbach, H., de Rosnay, P., Bell, B., Schepers, D., Simmons, A., Soci, C., Abdalla, S., Alonso-Balmaseda, M., Balsamo, G., Bechtold, P., Berrisfold, P., 2018. Operational global reanalysis: progress, future directions and synergies with NWP. ERA Rep. Ser. 106838, ECMWF. https://doi.org/10.21957/tkic6g3wm.

Hodgkins, G., Dudley, R.W. and Aichele, S.S., 2007. Historical changes in precipitation and streamflow in the US Great Lakes Basin, 1915-2004. US Geological Survey.

Homer, C., Dewitz, J., Yang, L., Jin, S., Danielson, P., Xian, G., Coulston, J., Herold, N., Wickham, J., Megown, K., 2015. Completion of the 2011 National Land Cover Database for the conterminous United States–representing a decade of land cover change information. Photogramm. Eng. Remote Sens. 81 (5), 345–354. https://doi.org/10.14358/PERS.81.5.345.

Hong, Y., Do, H.X., Kessler, J., Fry, L., Read, L., Nasab, A.R., Gronewold, A.D., Mason, L., Anderson, E.J., 2022. Evaluation of gridded precipitation datasets over international basins and large lakes. J. Hydrol. 607, 127507. https://doi.org/10.1016/j.jhydrol.2022.127507.

Hong, Y., Kessler, J., Titze, D., Yang, Q., Shen, X., Anderson, E.J., 2024. Towards efficient coastal flood modeling: a comparative assessment of bathtub, extended hydrodynamic, and total water level approaches. Ocean Dyn. 74, 391–405. https://doi.org/10.1007/s10236-024-01610-1.

Huang, S., Kumar, R., Flörke, M., Yang, T., Hundecha, Y., Kraft, P., Gao, C., Gelfan, A., Liersch, S., Lobanova, A., Strauch, M., 2017. Evaluation of an ensemble of regional hydrological models in 12 large-scale river basins worldwide. Clim. Change 141, 381–397. https://doi.org/10.1007/s10584-016-1841-8.

Johnson, F., Sharma, A., 2009. Measurement of GCM skill in predicting variables relevant for hydroclimatological assessments. J. Clim. 22 (16), 4373–4382. https://doi.org/10.1175/2009JCLI2681.1.

Johnston, C.A., Shmagin, B.A., 2008. Regionalization, seasonality, and trends of streamflow in the US Great Lakes Basin. J. Hydrol. 362 (1-2), 69–88. https://doi.org/10.1016/j.jhydrol.2008.08.010.

Kayastha, M.B., Ye, X., Huang, C., Xue, P., 2022. Future rise of the Great Lakes water levels under climate change. J. Hydrol. 612, 128205. https://doi.org/10.1016/j.jhydrol.2022.128205.

Khan, M.S., Liaqat, U.W., Baik, J., Choi, M., 2018. Stand-alone uncertainty characterization of GLEAM, GLDAS and MOD16 evapotranspiration products using an extended triple collocation approach. Agric. For. Meteorol. 252, 256–268. https://doi.org/10.1016/j.agrformet.2018.01.022.

Konapala, G., Mishra, A.K., Wada, Y., Mann, M.E., 2020. Climate change will affect global water availability through compounding changes in seasonal precipitation and evaporation. Nat. Commun. 11 (1), 3044. https://doi.org/10.1038/s41467-020-16757-w.

Kult, J.M., Fry, L.M., Gronewold, A.D., Choi, W., 2014. Regionalization of hydrologic response in the Great Lakes basin: Considerations of temporal scales of analysis. J. Hydrol. 519, 2224–2237. https://doi.org/10.1016/j.jhydrol.2014.09.083.

Lahmers, T.M., Gupta, H., Castro, C.L., Gochis, D.J., Yates, D., Dugger, A., Goodrich, D., Hazenberg, P., 2019. Enhancing the structure of the WRF-hydro hydrologic model for semiarid environments. J. Hydrometeorol. 20 (4), 691–714. https://doi.org/10.1175/JHM-D-18-0064.1.

Liu, L., Menenti, M., Ma, Y., 2022. Evaluation of albedo schemes in WRF coupled with Noah-MP on the Parlung No. 4 Glacier. Remote Sens. 14 (16), 3934. https://doi.org/10.3390/rs14163934.

Ljungqvist, F.C., Krusic, P.J., Sundqvist, H.S., Zorita, E., Brattström, G., Frank, D., 2016. Northern Hemisphere hydroclimate variability over the past twelve centuries. Nature 532 (7597), 94–98. https://doi.org/10.1038/nature17418.

Lofgren, B.M., Hunter, T.S., Wilbarger, J., 2011. Effects of using air temperature as a proxy for potential evapotranspiration in climate change scenarios of Great Lakes basin hydrology. J. Gt. Lakes Res. 37 (4), 744–752. https://doi.org/10.1016/j.jglr.2011.09.006.

Ma, N., Niu, G.Y., Xia, Y., Cai, X., Zhang, Y., Ma, Y., Fang, Y., 2017. A systematic evaluation of Noah-MP in simulating land-atmosphere energy, water, and carbon exchanges over the continental United States. J. Geophys. Res.: Atmos. 122 (22), 12–245. https://doi.org/10.1002/2017JD027597.

Mai, J., Shen, H., Tolson, B.A., Gaborit, É ., Arsenault, R., Craig, J.R., Fortin, V., Fry, L.M., Gauch, M., Klotz, D., Kratzert, F., 2022. The great lakes runoff intercomparison project phase 4: the great lakes (GRIP-GL). Hydrol. Earth Syst. Sci. 26 (13), 3537–3572. https://doi.org/10.5194/hess-26-3537-2022.

Mai, J., Tolson, B.A., Shen, H., Gaborit, É ., Fortin, V., Gasset, N., Awoye, H., Stadnyk, T.A., Fry, L.M., Bradley, E.A., Seglenieks, F., 2021. Great Lakes runoff intercomparison project phase 3: Lake Erie (GRIP-E). J. Hydrol. Eng. 26 (9), 05021020. https://doi.org/10.1061/(ASCE)HE.1943-5584.0002097.

Mailhot, E., Music, B., Nadeau, D.F., Frigon, A., Turcotte, R., 2019. Assessment of the Laurentian Great Lakes' hydrological conditions in a changing climate. Clim. Change 157, 243–259. https://doi.org/10.1007/s10584-019-02530-6.

Mao, D., Cherkauer, K.A., 2009. Impacts of land-use change on hydrologic responses in the Great Lakes region. J. Hydrol. 374 (1-2), 71–82. https://doi.org/10.1016/j.jhydrol.2009.06.016.

Martens, B., Miralles, D.G., Lievens, H., Van Der Schalie, R., De Jeu, R.A., Fernández-Prieto, D., Beck, H.E., Dorigo, W.A., Verhoest, N.E., 2017. GLEAM v3: satellite-based land evaporation and root-zone soil moisture. Geosci. Model Dev. 10, 1903–1925. https://doi.org/10.5194/gmd-10-1903-2017.

Mason, L.A., Gronewold, A.D., Laitta, M., Gochis, D., Sampson, K., Read, L., Klyszejko, E., Kwan, J., Fry, L., Jones, K., Steeves, P., 2019. New transboundary hydrographic data set for advancing regional hydrological modeling and water resources management. J. Water Resour. Plan. Manag. 145 (6), 06019004, 10.1061/(ASCE)WR.1943-5452.0001073.

Mason, L.A., Riseng, C.M., Gronewold, A.D., Rutherford, E.S., Wang, J., Clites, A., Smith, S.D., McIntyre, P.B., 2016. Fine-scale spatial variation in ice cover and surface temperature trends across the surface of the Laurentian Great Lakes. Clim. Change 138, 71–83. https://doi.org/10.1007/s10584-016-1721-2.

Maurer, G.E., Bowling, D.R., 2014. Seasonal snowpack characteristics influence soil temperature and water content at multiple scales in interior western US mountain ecosystems. Water Resour. Res. 50 (6), 5216–5234. https://doi.org/10.1002/2013WR014452.

Maurer, J.M., Schaefer, J.M., Rupper, S., Corley, A.J.S.A., 2019. Acceleration of ice loss across the Himalayas over the past 40 years. Sci. Adv. 5 (6), eaav7266. https://doi.org/10.1126/sciadv.aav7266.

McKay, L., Bondelid, T., Dewald, T., Johnston, J., Moore, R., Rea, A., 2012. *NHDPlus Version 2: User Guide*. US Environmental Protection Agency [online].

Méthot, J., Huang, X., Grover, H., 2015. Demographics and societal values as drivers of change in the Great Lakes–St. Lawrence River basin. J. Gt. Lakes Res. 41, 30–44. https://doi.org/10.1016/j.jglr.2014.11.001.

Miller, D.A. and White, R.A., 1998. A conterminous United States multilayer soil characteristics dataset for regional climate and hydrology modeling. Earth Interact. 2 (2), 1-26. doi: 10.1175/1087-3562(1998)002%3C0001:ACUSMS%3E2.3.CO;2.

Mishra, A.K., Özger, M., Singh, V.P., 2009. An entropy-based investigation into the variability of precipitation. J. Hydrol. 370 (1-4), 139–154. https://doi.org/10.1016/j.jhydrol.2009.03.006.

Monteith, J.L., 1965. Evaporation and Environment. In: In Symposia of the society for experimental biology, 19. Cambridge University Press, Cambridge, UK, pp. 205–234.

Moradkhani, H., 2008. Hydrologic remote sensing and land surface data assimilation. Sensors 8 (5), 2986–3004. https://doi.org/10.3390/s8052986.

Myers, D.T., Ficklin, D.L., Robeson, S.M., 2023. Hydrologic implications of projected changes in rain-on-snow melt for Great Lakes Basin watersheds. Hydrol. Earth Syst. Sci. 27 (9), 1755–1770. https://doi.org/10.5194/hess-27-1755-2023.

Nijssen, B., O'Donnell, G.M., Hamlet, A.F., Lettenmaier, D.P., 2001. Hydrologic sensitivity of global rivers to climate change. Clim. Change 50, 143–175. https://doi.org/10.1023/A:1010616428763.

Niu, G.Y., Yang, Z.L., Mitchell, K.E., Chen, F., Ek, M.B., Barlage, M., Kumar, A., Manning, K., Niyogi, D., Rosero, E., Tewari, M., 2011. The community Noah land surface model with multiparameterization options (Noah-MP): 1. Model description and evaluation with local-scale measurements. J. Geophys. Res.: Atmospheres 116 (D12). https://doi.org/10.1029/2010JD015139.

Pal, S., Wang, J., Feinstein, J., Yan, E., Kotamarthi, V.R., 2023. Projected changes in extreme streamflow and inland flooding in the mid-21st century over Northeastern United States using ensemble WRF-Hydro simulations. J. Hydrol.: Reg. Stud. 47, 101371. https://doi.org/10.1016/j.ejrh.2023.101371.

Ragettli, S., Pellicciotti, F., Immerzeel, W.W., Miles, E.S., Petersen, L., Heynen, M., Shea, J.M., Stumm, D., Joshi, S., Shrestha, A., 2015. Unraveling the hydrology of a Himalayan catchment through integration of high resolution in situ data and remote sensing with an advanced simulation model. Adv. Water Resour. 78, 94–111. https://doi.org/10.1016/j.advwatres.2015.01.013.

Rajib, M.A., Merwade, V., Yu, Z., 2016. Multi-objective calibration of a hydrologic model using spatially distributed remotely sensed/in-situ soil moisture. J. Hydrol. 536, 192–207. https://doi.org/10.1016/j.jhydrol.2016.02.037.
Rixen, C., Høye, T.T., Macek, P., Aerts, R., Alatalo, J.M., Anderson, J.T., Arnold, P.A., Barrio, I.C., Bjerke, J.W., Björkman, M.P., Blok, D., 2022. Winters are changing: snow effects on Arctic and alpine tundra ecosystems. Arct. Sci. 8 (3), 572–608. https://doi.org/10.1139/as-2020-0058.
Running, S.W., Mu, Q., Zhao, M., Moreno, A., 2017. User's Guide MODIS Global Terrestrial Evapotranspiration (ET) Product (MOD16A2/A3 and Year-end Gap-filled MOD16A2GF/A3GF) NASA Earth Observing System MODIS Land Algorithm (For Collection 6.1). Retrieved from https://landweb.modaps.eosdis.nasa.gov/QA_WWW/forPage/MODIS_C61_Land_.
Sen, P.K., 1968. Estimates of the regression coefficient based on Kendall's tau. J. Am. Stat. Assoc. 63 (324), 1379–1389. https://doi.org/10.1080/01621459.1968.10480934.
Shin, S., Gronewold, A.D., Fry, L., Dugger, A., Kessler, J., 2024. Evaluating surface and subsurface fluxes in hydrological models to advance basin-scale operational water supply forecasting. Hydrol. Sci. J. 1–18. https://doi.org/10.1080/02626667.2024.2378100.
Shin, S., Gronewold, A.D., 2024. University of Michigan - Deep Blue Data. Hydrol. Simul. Across Gt. Lakes Basin 1941 2020 [Data Set.]. https://doi.org/10.7302/wkd1-nb64.
Shin, S., Her, Y., Khare, Y., 2023a. Evaluation of impacts of climate change on natural and managed wetland basins. J. Am. Water Resour. Assoc. 59 (6), 1549–1568. https://doi.org/10.1111/1752-1688.13140.
Shin, S., Her, Y., Muñoz-Carpena, R., Yu, X., 2023b. Quantifying the contribution of external loadings and internal hydrodynamic processes to the water quality of Lake Okeechobee. Sci. Total Environ. 883, 163713. https://doi.org/10.1016/j.scitotenv.2023.163713.
Shrestha, N.K., Seglenieks, F., Temgoua, A.G., Dehghan, A., 2022. The impacts of climate change on land hydroclimatology of the Laurentian Great Lakes Basin. Front. Water 4, 801134. https://doi.org/10.3389/frwa.2022.801134.
Song, J.H., Her, Y., Shin, S., Cho, J., Paudel, R., Khare, Y.P., Obeysekera, J., Martinez, C.J., 2020. Evaluating the performance of climate models in reproducing the hydrological characteristics of rainfall events. Hydrol. Sci. J. 65 (9), 1490–1511. https://doi.org/10.1080/02626667.2020.1750616.
Soonthornrangsan, J.T., Lowry, C.S., 2021. Vulnerability of water resources under a changing climate and human activity in the lower Great Lakes region. Hydrol. Process. 35 (12), e14440. https://doi.org/10.1002/hyp.14440.
Staebler, R. 2022. AmeriFlux BASE CA-Cbo Ontario - Mixed Deciduous, Borden Forest Site, Ver. 6-5, AmeriFlux AMP, (Dataset). https://doi.org/10.17190/AMF/1498755.
Stahl, K., Tallaksen, L.M., Hannaford, J., Van Lanen, H.A.J., 2012. Filling the white space on maps of European runoff trends: estimates from a multi-model ensemble. Hydrol. Earth Syst. Sci. 16 (7), 2035–2047. https://doi.org/10.5194/hess-16-2035-2012.
Sterner, R.W., Keeler, B., Polasky, S., Poudel, R., Rhude, K., Rogers, M., 2020. Ecosystem services of Earth's largest freshwater lakes. Ecosyst. Serv. 41, 101046. https://doi.org/10.1016/j.ecoser.2019.101046.
Stevenson, S., Coats, S., Touma, D., Cole, J., Lehner, F., Fasullo, J., Otto-Bliesner, B., 2022. Twenty-first century hydroclimate: a continually changing baseline, with more frequent extremes. Proc. Natl. Acad. Sci. 119 (12), e2108124119. https://doi.org/10.1073/pnas.2108124119.
Vano, J.A., Nijssen, B., Lettenmaier, D.P., 2015. Seasonal hydrologic responses to climate change in the Pacific Northwest. Water Resour. Res. 51 (4), 1959–1976. https://doi.org/10.1002/2014WR015909.
Wang, H., Liu, J., Klaar, M., Chen, A., Gudmundsson, L., Holden, J., 2024. Anthropogenic climate change has influenced global river flow seasonality. Science 383 (6686), 1009–1014. https://doi.org/10.1126/science.adi9501.
Wang, S., Pan, M., Mu, Q., Shi, X., Mao, J., Brümmer, C., Jassal, R.S., Krishnan, P., Li, J., Black, T.A., 2015. Comparing evapotranspiration from eddy covariance measurements, water budgets, remote sensing, and land surface models over Canada. J. Hydrometeorol. 16 (4), 1540–1560. https://doi.org/10.1175/JHM-D-14-0189.1.
Wieder, W.R., Kennedy, D., Lehner, F., Musselman, K.N., Rodgers, K.B., Rosenbloom, N., Simpson, I.R., Yamaguchi, R., 2022. Pervasive alterations to snow-dominated ecosystem functions under climate change. Proc. Natl. Acad. Sci. 119 (30), e2202393119. https://doi.org/10.1073/pnas.2202393119.
Woldemeskel, F.M., Sharma, A., Sivakumar, B., Mehrotra, R., 2016. Quantification of precipitation and temperature uncertainties simulated by CMIP3 and CMIP5 models. J. Geophys. Res.: Atmospheres 121 (1), 3–17. https://doi.org/10.1002/2015JD023719.
Wu, K., Johnston, C.A., 2007. Hydrologic response to climatic variability in a Great Lakes Watershed: a case study with the SWAT model. J. Hydrol. 337 (1-2), 187–199. https://doi.org/10.1016/j.jhydrol.2007.01.030.
Wu, Y., Zheng, H., Zhang, B., Chen, D., Lei, L., 2014. Long-term changes of lake level and water budget in the Nam Co Lake Basin, central Tibetan Plateau. J. Hydrometeorol. 15 (3), 1312–1322. https://doi.org/10.1175/JHM-D-13-093.1.
Yang, Z., Qian, Y., Xue, P., Wang, J., Chakraborty, T.C., Pringle, W.J., Li, J., Chen, X., 2023. Moisture sources of precipitation in the Great Lakes Region: climatology and recent changes. p.e2022GL100682 Geophys. Res. Lett. 50 (5). https://doi.org/10.1029/2022GL100682.
Yucel, I., Onen, A., Yilmaz, K.K., Gochis, D.J., 2015. Calibration and evaluation of a flood forecasting system: utility of numerical weather prediction model, data assimilation and satellite-based rainfall. J. Hydrol. 523, 49–66. https://doi.org/10.1016/j.jhydrol.2015.01.042.
Zhang, B., Xia, Y., Long, B., Hobbins, M., Zhao, X., Hain, C., Li, Y., Anderson, M.C., 2020a. Evaluation and comparison of multiple evapotranspiration data models over the contiguous United States: implications for the next phase of NLDAS (NLDAS-Testbed) development. Agric. For. Meteorol. 280, 107810. https://doi.org/10.1016/j.agrformet.2019.107810.
Zhang, L., Zhao, Y., Hein-Griggs, D., Janes, T., Tucker, S., Ciborowski, J.J., 2020b. Climate change projections of temperature and precipitation for the Great Lakes basin using the PRECIS regional climate model. Apr 1 J. Gt. Lakes Res. 46 (2), 255–266. https://doi.org/10.1016/j.jglr.2020.01.013.
Zheng, C., Jia, L., Hu, G., 2022. Global land surface evapotranspiration monitoring by ETMonitor model driven by multi-source satellite earth observations. J. Hydrol. 613, 128444. https://doi.org/10.1016/j.jhydrol.2022.128444.